The Pattern and Timing of Biotic Recovery from the End-Permian Extinction on the Great Bank of Guizhou, Guizhou Province, China

JONATHAN L. PAYNE*
Department of Earth and Planetary Sciences, Harvard University, Cambridge, MA 02138, E-mail: jlpayne@stanford.edu

DANIEL J. LEHRMANN
Department of Geology, University of Wisconsin-Oshkosh, Oshkosh, WI 54901

JIAYONG WEI
Guizhou Bureau of Geology and Mineral Resources, Guiyang, Guizhou Province, P.R.C.

ANDREW H. KNOLL
Department of Organismic and Evolutionary Biology, Harvard University, Cambridge, MA 02138

PALAIOS, 2006, V. 21, p. 63–85 DOI 10.2110/palo.2005.p05-12p

*Microfacies analysis and point counts of thin sections from 608 hand samples were used to track changes in the abundance and diversity of fossil grains through the extended recovery interval following end-Permian mass extinction on the Great Bank of Guizhou (GBG)—an isolated Late Permian to Late Triassic carbonate platform in south China. Exposure of a two-dimensional cross-section of the platform permits the comparison of faunal patterns along an environmental gradient from shallow to deep water. The diverse Late Permian biota was dominated by calcareous sponges, crinoids, articulate brachiopods, foraminifera, and calcareous algae. In contrast, Early Triassic communities were dominated by mollusks, with increasing abundance of crinoids beginning in the Spathian. Increase in the diversity and abundance of fossils on the GBG was confined to a brief interval near the Spathian–Anisian boundary and concentrated along the platform margin. Later Middle Triassic diversification, the return of calcareous algae and calcareous sponges, and the appearance of scleractinian corals did not substantially alter the mollusk-crinoid-*Tubiphytes *assemblage before the end of the Middle Triassic. The low abundance of skeletal grains in Lower Triassic strata implies: (1) similarities in the relative contributions of micrite, microbialites, and oolites to Neoproterozoic carbonates result, at least in part, from the temporary removal of skeletal sinks for calcium carbonate; and (2) animals with hard skeletons remained at low abundance from the time of the end-Permian extinction through much of the Early Triassic.*

INTRODUCTION

Early Triassic ecosystems bear little resemblance to their Paleozoic counterparts, exhibiting an unprecedented taxonomic dominance by mollusks and a complementary decrease in the representation of sponges, crinoids, brachiopods, and other non-motile, epifaunal suspension feeders characteristic of Paleozoic ecosystems (Bambach et al., 2002). They also differ substantially from Middle Triassic assemblages, which herald the onset of more diverse communities that contain the seeds of later Mesozoic and modern shallow-marine ecosystems.

Extinction at the end of the Permian Period eliminated 67% of Late Permian marine genera and 56% of genera known from the latest Permian Changhsingian stage (see Sepkoski, 2002). The major extinction pulse occurred rapidly at the end of the Permian, in less (or much less) than 500 ky (Bowring et al., 1998; Rampino and Adler, 1998; Jin et al., 2000; Rampino et al., 2000), preferentially affecting animals with passive respiratory systems and heavy calcification (Knoll et al., 1996). Whereas the trigger and kill mechanisms remain controversial (see, e.g., Wignall and Hallam, 1992; Knoll et al., 1996; Becker et al., 2001; Basu et al., 2003; Becker et al., 2004), the selectivity of the extinction appears to account in large part for the post-extinction ecological revolution: heavily calcified organisms with passive respiratory systems also tend to be non-motile, epifaunal suspension feeders (e.g., brachiopods, crinoids, and sponges). Ecologically, as well as taxonomically, the extinction was the most severe of the Phanerozoic (McGhee et al., 2004).

Differences between Early and Middle Triassic ecosystems are not as well understood, and several obstacles have slowed progress in characterizing and interpreting the pattern of Triassic recovery. First, attention initially was focused on the extinction itself, rather than the recovery. Second, few expanded stratigraphic sections span the Early and Middle Triassic without a substantial change in depositional environment. Third, many Lazarus taxa (Jablonski, 1986) known to persist from the Late Permian to the Middle Triassic have never been observed within Lower Triassic strata (e.g., Batten, 1973; Erwin, 1996; Wignall and Benton, 1999; Twitchett et al., 2000; Wignall and Benton, 2000; Twitchett, 2001). Their absence may be due ei-

* Current address: *Department of Geological and Environmental Sciences, Stanford University, Stanford, CA 94305.*

Copyright © 2006, SEPM (Society for Sedimentary Geology) 0883-1351/06/0021-0063/$3.00

ther to changes in the abundance and size of organisms during the Early Triassic (Wignall and Benton, 1999; Twitchett, 2001; Payne, 2005) or to the poor quality of the Lower Triassic fossil record, resulting, for example, from the rarity of silicified Lower Triassic fossil assemblages (Schubert et al., 1997).

Consequently, much of what is known of the pattern of Triassic recovery is derived from compilations of taxonomic diversity on regional and global scales. For example, Sepkoski's (2002) database shows that global genus diversity remained static through the first half of the Early Triassic, then began to increase in the Smithian (late Early Triassic); the greatest diversity increase, however, did not occur until the Anisian (Sepkoski, 2002), at least 4 million years after the extinction (Martin et al., 2001). Independent studies of global gastropod diversity (Pan and Erwin, 1994; Erwin, 1996) and brachiopod diversity from southern China (Shen and Shi, 1996) parallel the pattern observed in Sepkoski's compilation.

Diversity within marine communities also was low throughout the Early Triassic (Schubert and Bottjer, 1995; Rodland and Bottjer, 2001). The most diverse assemblages known are dominated by ten or fewer genera of bivalves and gastropods (e.g., Twitchett et al., 2004), and some Griesbachian (earliest Triassic) bedding planes contain macrofaunal assemblages that consist nearly exclusively of a single taxon, such as the pectinid bivalve *Claraia* (Schubert and Bottjer, 1995) or the phosphatic brachiopod *Lingula* (Rodland and Bottjer, 2001). Generally, local communities were dominated by bivalves, gastropods, and, in the Spathian, echinoderms, showing very limited ecological and taxonomic diversity (Schubert and Bottjer, 1995) and universally lacking the large species of gastropods common in the Permian and Middle Triassic (Fraiser and Bottjer, 2004; Payne, 2005). Preliminary analyses indicate a comparable absence of large species across several higher taxa (Price-Lloyd and Twitchett, 2002).

Sedimentary features of Lower Triassic strata reinforce the impression of delayed Early Triassic recovery interpreted from taxonomic compilations. More than that, however, they record qualitative changes in fossil assemblages and sedimentary systems that suggest there is more to explain than low species richness. Metazoan reefs are absent from Lower Triassic rocks (Flügel, 1994); instead, stromatolites, thrombolite-like buildups, and seafloor carbonate precipitates are common in Lower Triassic shallow-marine shelf settings (e.g., Schubert and Bottjer, 1992; Baud et al., 1997; Lehrmann, 1999; Lehrmann et al., 2001; Lehrmann et al., 2003; Pruss, 2004). Two abundant groups of Permian fossils, calcareous algae (Flügel, 1985) and calcareous sponges (Riedel and Senowbari-Daryan, 1991), also are absent (or nearly absent) from Lower Triassic strata, although they reappear in Middle Triassic deposits. The only exceptions to this pattern are a red alga similar to *Gymnocodium*, reported from the Griesbachian Vardebukta Formation of Spitsbergen (Wignall et al., 1998), and the green alga "*Acicularia*," reported from the latest Spathian of northeastern Iran (Baud et al., 1991). Generally low levels of bioturbation (Twitchett, 1999; Pruss and Bottjer, 2004a) also are reflected by the occurrence of flat-pebble conglomerates (Wignall and Twitchett, 1999), and ribbon rock (Lehrmann et al., 2001), as well as the preservation of wrinkle structures derived from microbial mats in open-marine environments—a phenomenon largely restricted to hypersaline lagoonal environments through most of the Phanerozoic (Pruss et al., 2004).

Despite increasing attention to the Lower Triassic fossil record, the mechanism underlying the delayed recovery is poorly understood. Debate continues as to whether the slow recovery primarily reflects the magnitude of the extinction or, alternatively, resulted from persistent environmental inhibition. Stanley (1990) suggested that adverse climatic conditions slowed recovery, whereas Hallam (1991) and other workers (Wignall and Hallam, 1992, 1993, 1996; Woods et al., 1999; Rodland and Bottjer, 2001; Kidder and Worsley, 2004) have argued that anoxia and related oceanographic conditions delayed diversification. Erwin (1996, 1998) suggested that the magnitude of the extinction provides an alternative explanation for the slow recovery, and recent models of evolutionary diversification incorporating the effects of species-species interactions in diversity increase may help to explain an apparent lag between extinction and the interval of most rapid diversification (Erwin et al., 2004).

Ecological models, however, do not easily account for the sedimentary phenomena noted above, or for geochemical evidence suggesting fluctuating environmental conditions throughout the Early Triassic (see, e.g., Marenco et al., 2004; Newton et al., 2004; Payne et al., 2004). Formulating convincing tests of ecological versus environmental controls on recovery using the fossil and rock records has proven challenging. For example, it is attractive to interpret large Early Triassic carbon isotope fluctuations documented on the Great Bank of Guizhou (Payne et al., 2004) and elsewhere (Baud et al., 1996; Atudorei and Baud, 1997; Atudorei, 1999; Horacek et al., 2001) as evidence for continuing environmental disturbance, but they may reflect ecological control of the carbon cycle (Payne et al., 2004). Constraining scenarios that account for these long-term Early Triassic phenomena is important not only for understanding controls on recovery. If these conditions were set in place at the Permian–Triassic boundary, they also may help to constrain explanations for the extinction itself.

Distinguishing the roles of ecological and environmental factors in governing the recovery requires, at the very least, highly resolved paleontological records of recovery across the Permian–Triassic boundary and through the Early–Middle Triassic transition. By virtue of its well-preserved architecture as an isolated carbonate platform of Late Permian to Late Triassic age and its expanded stratigraphic sections, the Great Bank of Guizhou (GBG) is a nearly ideal place to examine the fossil record of the Triassic recovery. Lehrmann et al. (1998) documented the evolution of the platform from an isolated bank in the latest Permian to a low-relief bank rimmed by oolitic shoals in the Early Triassic, followed by a high-relief, reef- and escarpment-rimmed platform in the Middle Triassic (Lehrmann et al., 1998; figs. 7, 9, 11). Subsequent studies on the GBG have presented detailed descriptions of the facies found across the Permian–Triassic boundary (Lehrmann et al., 2003), including an investigation focused on the calcimicrobial facies (Lehrmann, 1999), as well as Lower Triassic peritidal cyclic facies found in the platform

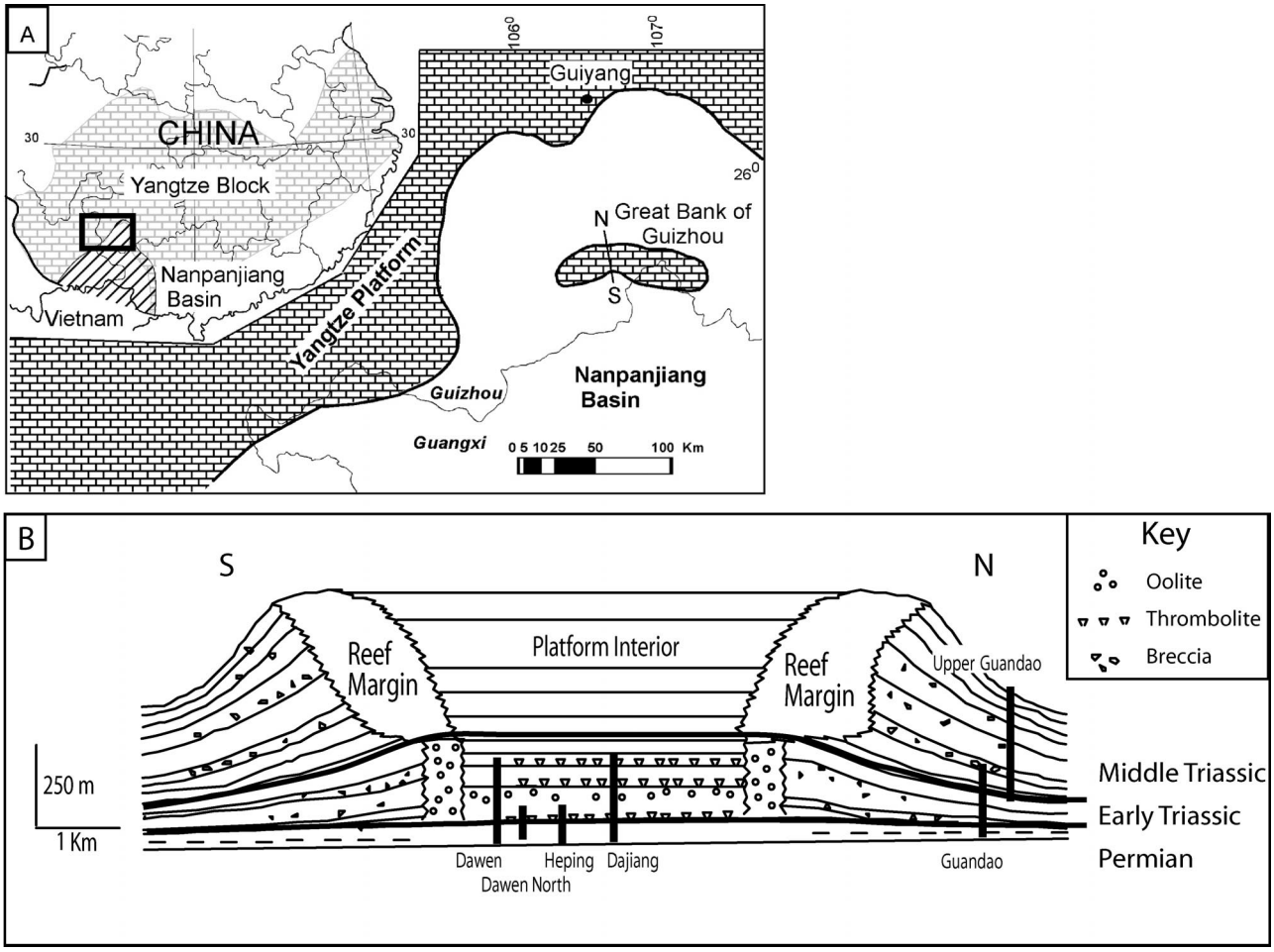

FIGURE 1—Schematic map of the study area. (A) Location map of the Great Bank of Guizhou (modified from Payne et al., 2004). (B) Schematic cross-section of the GBG. A symmetrical geometry is presented here, although the southern margin of the platform is not well exposed. Stratigraphic sections are marked with a black line, and names indicated.

interior (Lehrmann et al., 2001; Yang and Lehrmann, 2003).

In this study, environmental constraints provided by platform architecture and lithofacies are used to document the pattern of local faunal change across the end-Permian extinction and through the Early and Middle Triassic recovery interval, and across an environmental gradient from the platform interior to the basin margin. The ability to observe the entire recovery interval within a consistent environmental framework at a single geographic setting is rare due to the long duration of recovery. Fossil occurrences from the GBG, therefore, provide a high-quality dataset that can advance understanding of the patterns of Triassic recovery when compared with observations from other localities with more limited stratigraphic or environmental range.

GEOLOGICAL SETTING

The stratigraphic architecture of the platform has been the subject of detailed investigations previously (Lehrmann, 1993; Lehrmann et al., 1998), and therefore, is addressed only briefly here. The isolated platform formed in the Late Permian during drowning of the southern margin of the Yangtze Platform. Following retreat of the Yangtze Platform margin, a few topographic highs on the seafloor provided nuclei for isolated platforms, including the GBG. The GBG evolved from a low-relief bank with oolitic margins during the Early Triassic into a reef-rimmed, high-relief platform in the Middle Triassic before drowning and burial in siliciclastic basinal sediments in the Carnian (Lehrmann et al., 1998).

A faulted syncline between the towns of Bianyang and Bangun exposes a cross-section of the platform, with strata on the east limb of the syncline dipping to the west-southwest at approximately 60° (Fig. 1). Expanded and relatively complete stratigraphic sections are exposed from the platform interior and the basin margin, permitting comparison of recovery dynamics across an environmental gradient. The essentially continuous succession of shallow-subtidal to intertidal facies in the platform interior demonstrates that the platform provides a cross-section from shallow- to deep-water conditions throughout the study interval. Conodont biostratigraphic data and carbon isotopic data from previous work at the same localities (Payne et al., 2004) allow correlation among platform and basin sections and to more-distant localities.

A variety of lithofacies is represented within the GBG

platform architecture (Figs. 1, 2). Late Permian (Changhsingian) limestones of the Wujiaping Formation consist of cherty, fossiliferous grainstones and packstones both in the platform interior and on the basin margin. On the basin margin, these are overlain by the siliceous shales of the Dalong Formation. The end-Permian extinction horizon occurs at the top of the Wujiaping Formation in the platform interior, and at the top of the Dalong Formation on the basin margin. In the platform interior, a calcimicrobial horizon, 8–16 meters thick, that overlies the boundary horizon contains lenses of molluscan packstone and grainstone in most sections (Fig. 2). Overlying the calcimicrobial horizon is a thin, relatively diverse interval (by Lower Triassic standards) of packstone beds up to a few meters thick. The diverse packstone is overlain in turn by poorly fossiliferous lime-mudstones of the Daye Formation. Daye strata are overlain by dolomitized oolitic packstone, followed by cyclic peritidal facies (Fig. 2). The cyclic facies of the Lower Triassic platform interior consist of lime-mudstone, lime-packstone, oolites, calcimicrobialites, and flaser-bedded ribbon rock interpreted to represent repeated shallowing from shallow-subtidal to intertidal environments (discussed in detail by Lehrmann et al., 2001). Lower Triassic strata on the basin margin consist of unfossiliferous pelagic lime-mudstones and allodapic breccia units containing clasts of various lithofacies, predominantly oolites and lime-mudstones, but also occasional fossiliferous grainstones and packstones (Fig. 2). Beginning in the Spathian, strata on the basin margin are dominated by fossiliferous packstones and grainstones. Some of these packstones and grainstones exhibit graded bedding, reflecting turbidity-current transport of sediment downslope from the platform margin.

Approximately 600 meters of dolomitized shallow-water strata overlie the Lower Triassic cyclic interval in the platform interior. These strata span the interval from late Smithian to Anisian (Figs. 1, 2). Above the dolomitic interval, Middle Triassic platform-interior strata contain locally fossiliferous lagoonal and peritidal facies (Fig. 2). Contemporaneous basin-margin strata consist of fossiliferous grainstones and packstones, as well as breccia units containing blocks derived from a platform-margin reef complex. The Middle Triassic platform-margin reef complex (Fig. 1) also is well exposed and consists of *Tubiphytes* boundstones, crinoid and *Tubiphytes* grainstones, and large volumes of early marine cement.

METHODS

Six stratigraphic sections were measured on the GBG (Figures 1, 2). In the platform interior, the Dawen and Dajiang sections are Late Permian to Smithian (late Early Triassic), and the Dawen North and Heping sections cover the Permian–Triassic boundary interval. On the basin margin, the Guandao section exposes Late Permian–Anisian (Middle Triassic) strata, and the Upper Guandao section spans Spathian (late Early Triassic)–Carnian (Late Triassic) strata. The Middle Triassic part of the Dajiang section is more than 1 km thick, but logistically, it is challenging to sample due to mountainous terrain. Therefore, four intervals of the Middle Triassic strata within the Dajiang section, each approximately 20 meters thick, were sampled in detail to obtain representative data on platform-interior facies from the Middle Triassic strata. Sample spacing within all sections was one meter or less where exposure permitted; additional samples were collected from beds and intervals of particular interest. In total, more than 1200 samples were collected. More than 150 samples also were collected from the Middle Triassic reef margin. Their stratigraphic and geographic positions on the platform were determined using topographic maps and GPS. Many clasts within Lower Triassic breccias exposed on the basin margin are derived from the platform margin, and therefore provide an indirect sample of the poorly exposed Lower Triassic platform margin.

The difficulty of removing and identifying small shells from the clean platform limestones is a significant obstacle to detailed taxonomic investigation of those fossils not easily classified from thin sections. Because the primary goal of this study was an understanding of the local recovery pattern with high stratigraphic resolution, the pattern of biotic recovery was investigated primarily using thin sections. This approach sacrifices taxonomic resolution, but it has several compensating strengths. It provides much greater stratigraphic resolution than could be obtained with a more conventional taxonomic approach, especially in well-lithified strata lacking significant exposure of bedding planes. The use of thin sections also allows for accurate comparison of abundance, in terms of preserved skeletal volume, among taxa of widely varying sizes and across a great taxonomic range. Additionally, thin-section analysis also makes comparisons of abundance possible among taxa that contain easily identifiable specimens (e.g., gastropods) and those that either disarticulate (e.g., crinoids) or are too small to be counted in conventional studies (e.g., foraminifera, ostracodes). It further facilitates standardized sampling by allowing the investigator to search the same rock area in each sample and to take samples in the field at standard intervals because high-quality exposure of bedding planes and easily disaggregated lithologies are not required. Point-counting also has the benefit of providing quantitative sedimentological data on rock composition in conjunction with fossil-abundance data. Furthermore, this method allows one to quantify the abundance of fossil grains as a fraction of rock volume, providing a metric that potentially can track changes in the absolute abundance of skeletal animals in benthic marine communities.

Data from thin sections can present quite a different picture of a fossil community than data from specimen counts. For example, Jaanusson (1972) showed that counts of identifiable specimens in an Ordovician limestone from Sweden did not include any crinoids, despite the fact that these fossils contributed approximately half of the skeletal grains in the rock. Cephalopods, the majority of body fossils identifiable at the genus level, contributed an insignificant fraction (just a few percent) of the skeletal sediment. Although this example is extreme, it highlights the fact that point-count data from thin sections provide complementary information to taxonomic data; together, these approaches can provide a more complete understanding of the ecological structure of fossil communities than either could alone.

Thin sections were first surveyed for all identifiable fossils, and these were recorded at the lowest taxonomic level to which they could be assigned confidently. The level of

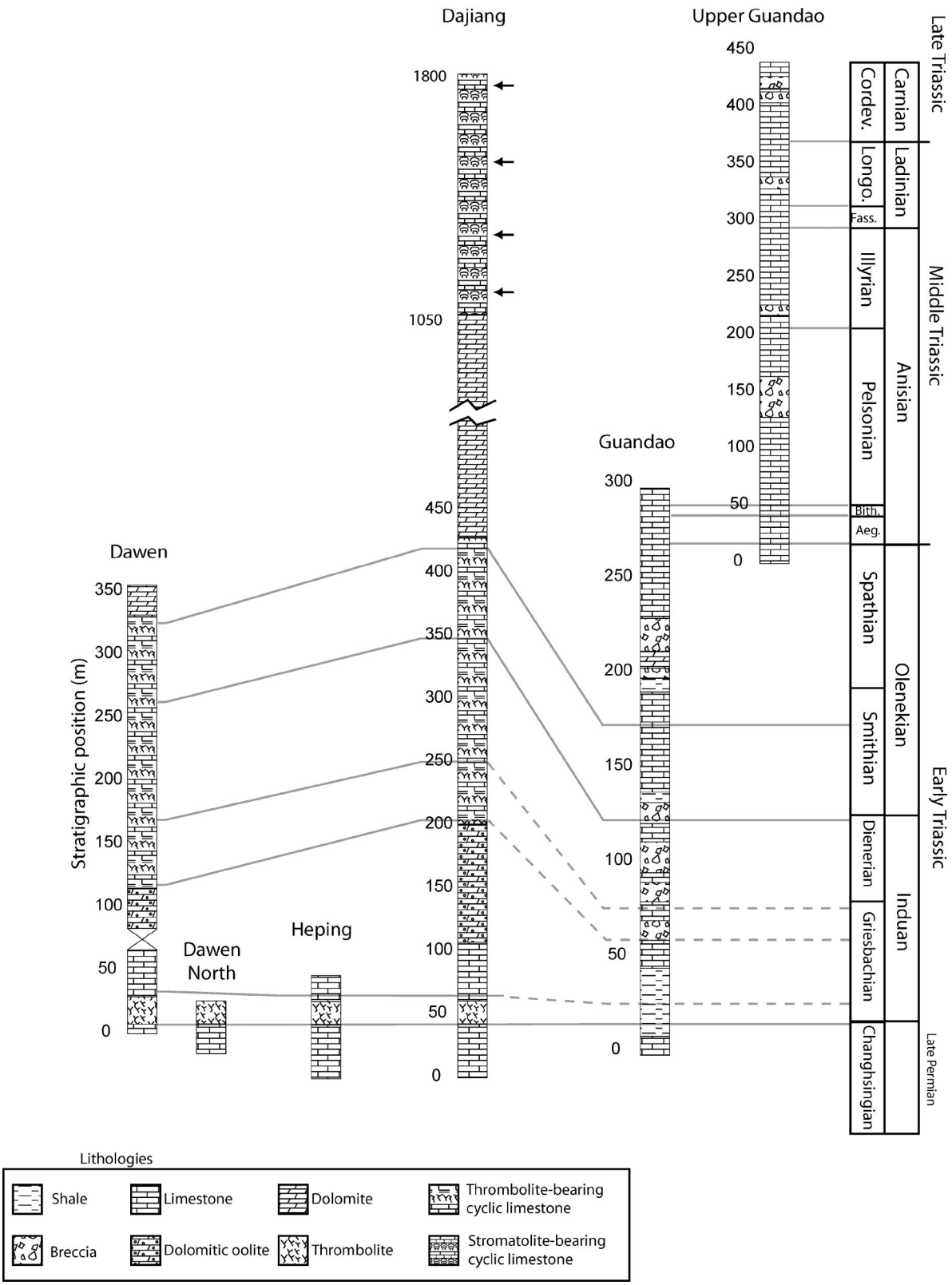

FIGURE 2—Stratigraphic columns of measured sections. Timescale is constrained by conodont occurrence data from the Guandao and Upper Guandao sections, and physical stratigraphic and carbon isotope correlations between the basin margin and the platform interior. Arrows indicate the positions of short sections sampled in detail from the Middle Triassic platform interior at Dajiang. Aeg. = Aegean; Bith. = Bithynian; Fass. = Fassanian; Longo. = Longobardian; Cordev. = Cordevolian.

TABLE 1—Taxonomic categories used in surveys of thin sections.

Major category	Subdivisions
Foraminiferan	Genus
Bryozoan	
Articulate Brachiopod	
Lingulid Brachiopod	
Bivalve	Pectinid, Non-Pectinid, Ornamented (non-pectinid)
Gastropod	Shape: low spired, medium spired, high spired, planispiral Ornamentation: smooth shell, ornamented
Cephalopod	
Ostracode	
Trilobite	
Echinoderm	Crinoid, Echinoid
Annelid	
Rugose coral	
Scleractinian coral	
Sponge	Sphinctozoan, Inozoan, Spicules
Solenoporacean	
Dasycladacean alga *Tubiphytes*	Vermiporellid, Teutloporellid, Round

taxonomic resolution varied by fossil type, ranging from genus level for foraminifera (based upon Salaj et al., 1983; Köylüoglu and Altiner, 1989; Kobayashi, 1997; Pronina-Nestell and Nestell, 2001; and other sources) to phylum or class level for several other groups (see Table 1). Abundance data were compiled from all thin sections from the Dajiang and Guandao sections, the Middle Triassic platform margin, and subsets of thin sections from the Dawen and Upper Guandao sections and the Middle Triassic reef complex. Counts of 300 points per sample were performed following the grain-solid method (Flügel, 1982) using a mechanical stage that stepped the slide at fixed increments. The grain-solid method is the standard point-counting technique for determining the volumetric composition of a rock. In this method, grains or matrix material that fall directly under the cross-hairs of the eyepiece are counted. Void space within a skeletal grain, therefore, is counted as the material that is filling the void (e.g., micrite or sparry calcite) rather than as part of the shell. Considering the effect of irregularly shaped and hollow fossil grains on the packing of skeletal material, very few rocks contain more than 50% skeletal material.

Six hundred and eight samples were prepared as thin sections, and surveyed for fossil content, non-skeletal grains, and sedimentary fabrics. Of these, 512 contained fossils. Taxonomic lists of identified fossils are presented at the stage level in Appendix 1 (http://www.sepm-org.archive.index.html), the lowest taxonomic resolution that could be determined with confidence (complete data on fossil diversity and abundance for each sample are available as a supplemental data file at http://www.sepm-org.archive.index.html). From the 608 samples, a subset of 349 samples was selected for point-counting to determine the volumetric contribution of skeletal and non-skeletal materials to the platform sediment. This subset included all thin sections from the Dajiang and Guandao sections, alternate thin-sections from the Upper Guandao section, and every fourth sample from the Dawen section. The abundance of fossils and fossil types can depend strongly on lithology and lithofacies type. Consequently, point-count data were tabulated by lithofacies, and the relative thicknesses of lithofacies within the stratigraphic sections (see Tables 2 and 3) were used as weighting factors to determine the mean fossil content at the substage level. Mean fossil abundance for individual lithofacies in the platform interior is shown in Table 4. Intervals of shale and massive dolomite were excluded from the analysis. The shale was too heavily weathered in most exposures to obtain samples conducive to thin sectioning. Strongly dolomitized intervals contained little recognizable primary fabric and were excluded because the original fossil content could not be ascertained.

RESULTS

The abundance of skeletal and non-skeletal materials in the limestone is tabulated for the platform interior in Table 5, platform margin in Table 6, and basin margin in Ta-

TABLE 2—Relative thicknesses of lithofacies in the platform interior (in percent). Ribbon rock consists of laminated and flaser-bedded interlayers of lime mudstone and grainstone, interpreted to represent muddy tidal-flat deposition (Lehrmann et al., 2001). MW = mudstone/wackestone; PG = packstone/grainstone; TH = thrombolite; OOL = oolite; RR = ribbon rock; DOL OOL = dolomitized oolite; DOL = dolomite.

	MW	PG	TH	OOL	RR	DOL OOL	DOL
Dawen							
Smithian	75.2	11.9	3.3	6.7	0.0	0.0	2.9
Dienerian	45.0	5.6	10.8	11.5	13.7	6.4	7.0
Griesbachian	64.5	12.7	22.4	0.4	0.0	0.0	0.0
Changhsingian	0.0	100.0	0.0	0.0	0.0	0.0	0.0
Dajiang							
Smithian	47.9	1.8	0.7	7.9	0.7	0.0	41.1
Dienerian	30.5	4.9	4.6	8.2	8.0	15.2	28.6
Griesbachian	74.2	3.7	22.1	0.0	0.0	0.0	0.0
Changhsingian	8.4	91.6	0.0	0.0	0.0	0.0	0.0
Mean platform interior							
Smithian	61.6	6.9	2.0	7.3	0.4	0.0	22.0
Dienerian	37.8	5.3	7.7	9.9	10.9	10.8	17.8
Griesbachian	69.4	8.2	22.3	0.2	0.0	0.0	0.0
Changhsingian	4.2	95.8	0.0	0.0	0.0	0.0	0.0

TABLE 3—Relative thicknesses of lithofacies on the basin margin (in percent). MW = mudstone/wackestone; PG = packstone/grainstone; BR = allodapic breccia.

	MW	PG	BR
Upper Guandao			
Carnian	0.0	36.5	63.5
Ladinian	0.0	86.0	14.0
Anisian	0.0	66.7	33.3
Spathian	10.5	75.7	13.8
Guandao			
Anisian	0.0	97.0	3.0
Spathian	43.2	50.8	6.0
Smithian	61.2	2.6	36.2
Dienerian	22.6	0.0	77.4
Griesbachian	58.2	0.0	41.8
Changhsingian	32.4	67.6	0.0

ble 7. The results are described in temporal sequence below to convey a brief summary of the patterns and trends observed. The ages for all samples are constrained by conodont biostratigraphy from the Guandao and Upper Guandao sections. Correlation to the platform interior is constrained by conodont biostratigraphy (principally around the Permian-Triassic boundary), physical tracing of beds, and carbon isotope stratigraphy (Payne et al., 2004).

Changhsingian

Changhsingian (Latest Permian) platform-interior strata consist of diverse skeletal grainstones and packstones containing abundant foraminifera, calcareous sponges, calcareous algae, solitary rugose corals, and echinoderms (online Appendix; Fig. 3 A–C). Thinner, interbedded wackestones contain a similar fauna. On the basin margin, the skeletal content is much lower and is dominated by sponge spicules, bryozoans, and brachiopods, with subordinate radiolarians (online Appendix). Cephalopods also were observed in the field, although they were not encountered in thin section. More than 30% of the overall rock volume in the platform interior and more than 7% on the basin margin is composed of skeletal material. All samples contain significant quantities of skeletal grains. The most abundant skeletal grains in the platform interior derive from calcareous sponges, echinoderms, dasyclad algae, foraminifera, and *Tubiphytes* (Table 5). Sponges, brachiopods, echinoderms, and bryozoans contributed most of the biotic grains in basin-margin sediments (Table 7). The number of distinguishable taxa is high in all stratigraphic sections, as exemplified by the many genera of foraminifera observed (online Appendix). Even within individual thin sections of Permian carbonates, the number of distinguishable taxa commonly reaches or exceeds the aggregate diversity of Griesbachian, Dienerian, and Smithian stratigraphic sections (Fig. 4). Furthermore, even those Changhsingian platform-interior samples and (most) basin-margin samples with the lowest skeletal abundances contain a higher proportion of skeletal sediment than the vast majority of Griesbachian, Dienerian, or Smithian samples from the same part of the platform (Fig. 4).

Griesbachian

The abundance and diversity of skeletal grains within Griesbachian samples are much lower than for Changhsingian samples. Skeletal grains comprise only 1.1% of the total rock volume in the platform interior and essentially are absent from samples of platform-margin and basin-margin strata (Tables 5–7; Fig. 3D–F). Breccia clasts derived from the platform margin consist primarily of oolites. Ooids alone contribute 42% of the rock volume in the sampled breccia clasts (Table 6). In the platform interior, mollusk shells are the dominant skeletal component. Bivalves and gastropods each compose over 40% of the identifiable metazoan skeletal material, and most of the unidentifiable fragments are likely molluscan in origin. Echinoderms, annelids, and phosphatic and articulate brachiopods also make measurable contributions to the skeletal biota, but they are confined primarily to a thin, diverse skeletal packstone unit immediately overlying calcimicrobial biostromes above the Permian–Triassic boundary (Fig. 2). Ostracodes do not make a significant volumetric contribution to the sediment, but are observed in a high proportion of the samples. Calcareous algae are entirely absent, and foraminifera are so small and rare that they were not registered during point-counts. On the scale of individual samples, the diversity and abundance of fossil grains in Griesbachian samples rarely reach the mean values for environmentally similar Changhsingian samples (Fig. 4).

Dienerian

The composition and abundance of biotic clasts in Dienerian samples from the platform interior are very similar to those of Griesbachian samples (online Appendix, Tables 5–7; Fig. 5A–C). The skeletal content of the platform-interior strata is extremely low (1.4%; Table 5), and is

TABLE 4—Skeletal abundances by lithofacies in the platform interior. See Table 2 for abbreviations. Note: lithofacies assignments were made in the field, rather than based on point-count results.

	Changhsingian	Griesbachian	Dienerian	Smithian	Middle triassic
MW	20.4	0.1	0.6	0.7	0.5
PG	31.8	10.4	8.5	0.6	0.8
TH		0.6	3.3	0.3	
RR			1.1		
OOL			0.5	1.1	
DOL OOL			0.0		
DOL			0.0	0.0	

TABLE 5—Relative abundance of biotic and abiotic components in platform interior limestones (in percent). In some cases, elements of the fauna are present in trace quantities such that they were identified in thin section, but were not among the points counted. These elements are marked with an asterisk.

	Changhsingian	Griesbachian	Dienerian	Smithian	Middle triassic
Sparry calcite	29.9	15.9	19.1	10.6	22.0
Micrite	37.4	78.4	64.5	72.6	68.8
Micritic clasts	1.4	0.1	0.9	0.5	6.6
Recrystallized clasts	0.0	0.1	5.8	9.8	0.8
Peloids	0.0	0.1	0.7	3.3	1.0
Microcrystalline cement	0.1	0.1	0.0	0.0	0.0
Fibrous cement	0.5	0.1	0.0	0.0	0.0
Syntaxial cement	0.1	0.0	0.0	0.0	0.0
Ooids	0.0	0.0	6.5	1.4	0.0
Microbial framework	0.0	4.2	1.0	1.2	0.0
Algae	2.8	0.0	0.0	0.0	0.0
Metazoa	14.0	0.8	1.0	0.5	0.3
Foraminifera	2.6	0.0*	0.0*	0.0*	0.0
Unidentifiable biotic	9.0	0.3	0.4	0.2	0.4
Tubiphytes	2.1	0.0	0.0	0.0	0.0
Identifiable biotic					
Algae & *Tubiphytes*	22.8	0.0	0.0	0.0	14.2
Metazoa	65.2	100.0	99.5	92.4	78.6
Foraminifera	12.1	0.0*	0.5	7.6	7.2
Metazoa					
Echinoderms	27.9	4.7	0.0	0.0	9.2
Bivalves	0.5	43.7	51.3	15.8	27.2
Gastropods	1.8	38.3	30.3	64.6	54.4
Ostracodes	1.2	1.2	15.2	17.3	9.2
Brachiopods	3.9	9.0	0.5	2.3	0.0
Other (Sponges, Corals, Cephalopods, Annelids, Trilobites)	64.6	3.1	2.7	0.0	0.0

TABLE 6—Relative abundance of biotic and abiotic components in platform-margin limestones (in percent). Griesbachian, Dienerian, Smithian, and Spathian data are derived from clasts in allodapic breccia units exposed in the Guandao section. Anisian data are derived from *in-situ* samples of the platform-margin reef complex.

	Griesbachian	Dienerian	Smithian	Spathian	Anisian
Sparry calcite	10.7	12.1	15.4	4.2	22.4
Micrite	36.0	63.1	65.8	85.2	13.5
Micritic clasts	5.1	3.2	6.3	6.4	2.1
Recrystallized clasts	0.0	1.8	2.7	0.0	0.0
Peloids	5.9	0.0	0.0	0.0	0.0
Microcrystalline cement	0.0	0.0	0.0	0.0	23.7
Fibrous cement	0.0	0.0	0.0	0.0	27.5
Syntaxial cement	0.0	0.0	0.0	0.0	0.0
Ooids	42.3	16.5	9.4	0.0	0.0
Microbial framework	0.0	0.0	0.0	0.0	0.0
Algae	0.0	0.0	0.0	0.0	2.3
Metazoa	0.0	2.7	0.2	3.0	1.4
Foraminifera	0.0	0.0	0.0	0.2	0.0
Unidentifiable biotic	0.0	0.6	0.2	1.0	0.2
Tubiphytes	0.0	0.0	0.0	0.0	6.9
Identifiable biotic					
Algae & *Tubiphytes*	No biota	0.0	0.0	0.0	62.2
Metazoa	No biota	100.0	89.2	95.1	37.8
Foraminifera	No biota	0.0	10.8	4.9	0.0
Metazoa					
Echinoderms	No biota	0.0	37.4	84.6	76.3
Bivalves	No biota	74.0	50.5	7.7	16.9
Gastropods	No biota	20.8	0.0	0.0	1.7
Ostracodes	No biota	1.3	12.1	7.7	0.0
Brachiopods	No biota	0.0	0.0	0.0	1.7
Other (Sponges, Corals, Cephalopods, Annelids, Trilobites)	No biota	3.9	0.0	0.0	3.4

TABLE 7—Relative abundance of biotic and abiotic components in basin-margin limestones (in percent). In some cases, elements of the fauna are present in trace quantities, such that they were identified in thin section but were not among the points counted. These elements are marked with an asterisk.

	Changh-singian	Gries-bachian	Dienerian	Smithian	Spathian	Anisian	Ladinian	Carnian
Sparry calcite	1.6	1.5	1.5	5.6	15.0	24.1	30.5	37.8
Micrite	88.0	98.3	98.1	91.8	68.8	43.6	37.7	19.3
Micritic clasts	0.0	0.1	0.1	1.0	8.0	21.6	25.8	31.9
Recrystallized clasts	3.0	0.0	0.0	0.0	0.1	0.5	0.4	2.9
Peloids	0.0	0.0	0.2	0.4	2.8	0.2	0.0	0.0
Microcrystalline cement	0.0	0.0	0.0	0.0	0.0	0.5	0.0	0.6
Fibrous cement	0.0	0.0	0.0	0.0	0.0	0.1	0.0	0.0
Syntaxial cement	0.0	0.0	0.0	0.0	0.1	0.1	0.0	0.1
Ooids	0.0	0.0	0.0	0.0	0.0	0.0	0.0	0.0
Microbial framework	0.0	0.0	0.0	0.0	0.0	0.1	0.0	0.0
Algae	0.1	0.0	0.0	0.0	0.0	0.2	0.0	0.1
Metazoa	4.6	0.0*	0.1	0.0*	3.9	3.5	2.8	3.2
Foraminifera	0.0*	0.0	0.0	0.0*	0.1	0.1	0.1	0.0*
Unidentifiable biotic	2.7	0.0	0.0	1.2	1.1	1.4	0.9	1.4
Tubiphytes	0.0	0.0	0.0	0.0	0.1	4.1	1.8	2.7
Identifiable biotic								
Algae & *Tubiphytes*	2.5	0.0	0.0	0.0	2.9	54.3	38.1	46.3
Metazoa	97.5	100.0	100.0	100.0	95.8	44.2	60.3	53.7
Foraminifera	0.0	0.0	0.0	0.0	1.4	1.5	1.6	0.0
Metazoa								
Echinoderms	8.9	50.0	0.0	66.7	62.5	72.5	53.9	48.3
Bivalves	0.5	0.0	100.0	33.3	27.5	13.6	39.5	27.6
Gastropods	0.0	0.0	0.0	0.0	0.0	1.9	1.3	3.4
Ostracode	2.5	0.0	0.0	0.0	4.1	3.4	2.6	3.4
Brachiopod	16.3	50.0	0.0	0.0	3.9	8.3	2.6	3.4
Other (Sponges, Corals, Cephalopods, Annelids, Trilobites)	71.7	0.0	0.0	0.0	2.0	0.2	0.0	13.8

dominated by bivalves and gastropods. Similarly to Griesbachian strata, gastropods and bivalves comprise over 80% of the identifiable skeletal material. Ostracodes, foraminifera, annelids (serpulids and spirorbids), and brachiopods also are present, but only ostracodes contribute more than a few percent of the identifiable skeletal material (Table 5). The skeletal content of basin-margin strata is near zero. The higher skeletal content of the platform margin in the Dienerian largely reflects two fossiliferous molluscan packstone clasts sampled from breccias on the basin margin (Table 6). Unlike the stratigraphic sections, the breccia units were not sampled at regular intervals or in a random fashion. Rather, fossiliferous clasts were selected preferentially to obtain a picture of the platform-margin biota. For this reason, the reported skeletal content of the platform margin likely overestimates significantly the mean skeletal content of platform-margin strata *in situ* because of this non-random sampling strategy. There is little evidence in the samples of a benthic or pelagic basinal biota. Although the skeletal content of the fossiliferous samples is high, the rarity of such clasts within breccia units suggests that a few molluscan banks existed along a predominantly oolitic platform margin.

Smithian

Smithian platform-interior strata contain a similar biota to that found in the Griesbachian and Dienerian (online Appendix; Fig. 5D–F). Gastropods dominate the fauna, with significant contributions from bivalves and ostracodes and minor contributions from foraminifera and brachiopods (Table 5). The skeletal biotic contribution to platform sediments is low (<1%). Identifiable microbial framework in the thrombolitic units contributes another 1.2% of the sediment volume. This value is a conservative one because the microbial framework is prone to recrystallization, which renders it unidentifiable. Basin-margin samples from the Guandao section also exhibit a very low skeletal abundance (0.3%), consisting of echinoderms and bivalves (Table 7). Samples of breccias representing the platform margin contain a similar fauna dominated by bivalves and crinoids with minor ostracodes, also in low abundance (Table 6). The echinoderm material, mostly crinoids, occurs as loose grains within grainstones and breccias, indicating that crinoids lived on or basinward of the platform margin. These samples provide the first indication of a substantial change in the biota since the Permian–Triassic boundary. The extremely low abundance and diversity of biotic material in all environments during the Smithian, however, suggest that measurable biotic recovery from the end-Permian extinction had yet to affect the GBG at the end of the Smithian.

Spathian

Spathian platform-margin and basin-margin strata contain a substantially greater abundance of skeletal material and higher diversity than underlying Lower Triassic rocks. Biotic clasts constitute 5.1% of the basin-margin sediment and 4.2% of breccias derived from the platform

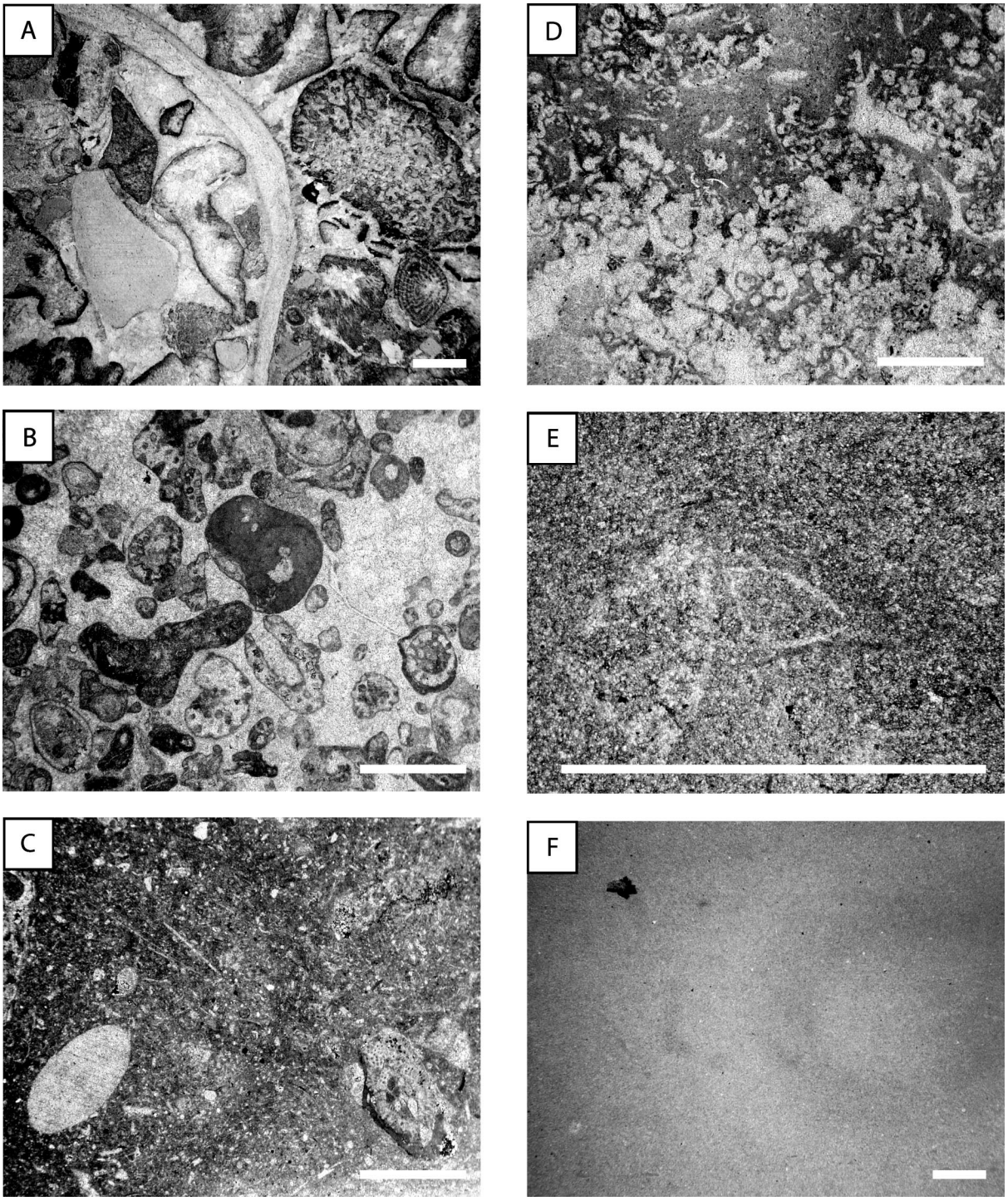

FIGURE 3—Photomicrographs of representative Permian and Griesbachian samples. All scale bars are 2 mm. (A) Changhsingian skeletal grainstone containing an articulate brachiopod, inozoan sponge, fusulinid foraminiferan, and echinoderm fragment, from the Dajiang section (PDJ-30), representing the platform facies. (B) Changhsingian skeletal grainstone containing dasycladacean algae and *Tubiphytes* from the basin-margin Heping section (HP-47). (C) Changhsingian skeletal packstone containing sponge spicules, a crinoid ossicle, and a bryozoan, Guandao section (PGD-2). (D) Griesbachian calcimicrobial boundstone containing microbial framework, micritic sediment fill, and ostracodes, Dawen North section (PND-7K). (E) Griesbachian carbonate wackestone containing small articulate brachiopods from the platform-interior Dajiang section (PDJ-64). (F) Unfossiliferous Griesbachian carbonate mudstone from the basin-margin Guandao section (PGD-18).

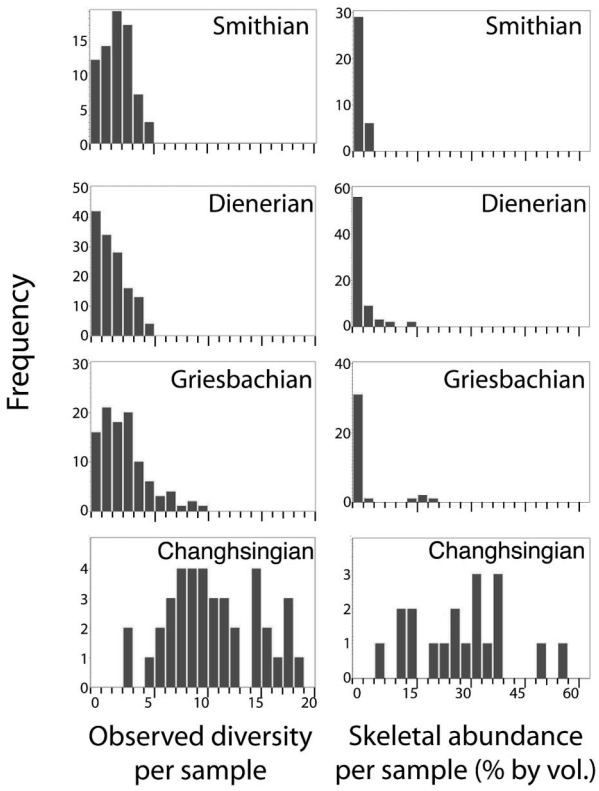

FIGURE 4—Histograms of diversity (left column) and fossil abundance (right column) observed within platform-interior samples from the Changhsingian through the Smithian.

margin. Echinoderms, particularly crinoids, dominate the skeletal component, which also includes bivalves, cephalopods, foraminifera, brachiopods, ostracodes, and the microproblematicum *Tubiphytes* in both platform-margin and basin-margin settings. *Tubiphytes* is not a skeleton analogous to a bivalve or gastropod shell, or even the preserved carbonate skeleton of a dasyclad alga. Rather, this problematic fossil may consist primarily of micritic cement deposited in association with an alga, perhaps induced by an enveloping microbial community (Senowbari-Daryan and Flügel, 1993). Regardless of its origin, however, *Tubiphytes* constitutes a significant component of the rock volume and provides much of the structure found in the Anisian reef complex. Rare fragments of *Tubiphytes* are first found in uppermost Spathian strata, only a few meters below the base of the Anisian. In this study, the Spathian–Anisian boundary is defined by the first occurrence of *Chiosella timorensis*, the conodont that likely will be used to define the boundary in the GSSP section (Ogg, 2004). The occurrence of these *Tubiphytes* fragments below the Spathian–Anisian boundary suggests that the platform-margin reef complex had initiated by this time, making it among the oldest, if not the oldest, known from Triassic strata (see, e.g., Flügel, 2002). The increased diversity of foraminifera (online Appendix) may indicate diversification at lower taxonomic levels within other taxa as well. Spathian samples from the basin margin demonstrate a significant increase in skeletal contribution to sediment accumulation and a change in the composition of the biota (Tables 6, 7; Fig. 6A–C). Pervasive dolomitization of Spathian platform-interior strata prevented analysis of samples from the Dajiang and Dawen sections. Subdivision of the Spathian at the Guandao section into three stratigraphic intervals, each represented by ten samples, indicates that the abundance of metazoan skeletal material increased gradually throughout the Spathian on the basin margin, as can be seen in Figure 7. At this fine stratigraphic scale, it is difficult to differentiate the effects of changes in the sedimentation rates from an increase in the rate of production of biotic grains, but these observations suggest a gradual increase in the abundance of the platform-margin biota.

Anisian

The abundance and composition of skeletal grains characteristic of the Middle Triassic within basin-margin sediments were established within the Aegean, the first substage of the Anisian. When the Middle Triassic data are tabulated by stage, there is no trend in the abundance or composition of biotic clasts on the basin margin from the Aegean to the Longobardian at the end of the Ladinian and the Cordevolian at the beginning of the Carnian (Figs. 7–9). This interval represents more than 10 million years based upon recent dates at the Spathian–Anisian boundary (Martin et al., 2001), within the Middle Triassic (Mundil et al., 1996; Muttoni et al., 2004b), and within the Late Triassic (Muttoni et al., 2004a). Crinoids contributed the greatest fraction of grains among the metazoa, followed by bivalves.

Tubiphytes was the most abundant framework element within the platform-margin reef complex in the Anisian, and *Tubiphytes* grains are significant components of basin-margin grainstones and packstones (Tables 6, 7; Fig. 6D–F). The skeletal content of the basin-margin strata approximately doubled, reaching 8.6% in the Guandao section and 9.8% in the Upper Guandao section. The taxonomic composition of metazoan skeletal material, however, did not change appreciably from Spathian levels, continuing to consist predominantly of crinoid fragments (Fig. 9). The slightly higher proportion of echinoderm debris and lower content of *Tubiphytes* in the more basinal Upper Guandao section may reflect the distribution of crinoids primarily along the margin of the platform, basinward of the reef complex (Fig. 1B). In addition to the changes in abundance and composition of biotic clasts, it appears that the maximum size of many taxa, particularly gastropods and crinoids, increased substantially during the Anisian. Gastropods observed in the platform interior reach heights of up to 15 cm and routinely are larger than the largest known specimens from the Early Triassic worldwide (Nützel, 2005; Payne, 2005). The earliest Middle Triassic occurrence of a dasyclad alga on the GBG is within the Pelsonian. One possible specimen of a scleractinian coral was observed higher in Pelsonian strata, but the first unambiguous specimens occur in Ladinian rocks. The oldest calcareous sponges on the GBG are found within the Anisian reef complex. The first occurrences of all of these organisms locally correlate with or are slightly younger than the first occurrences known for the groups globally in the Triassic (Ott, 1972; Senowbari-Daryan et al., 1993).

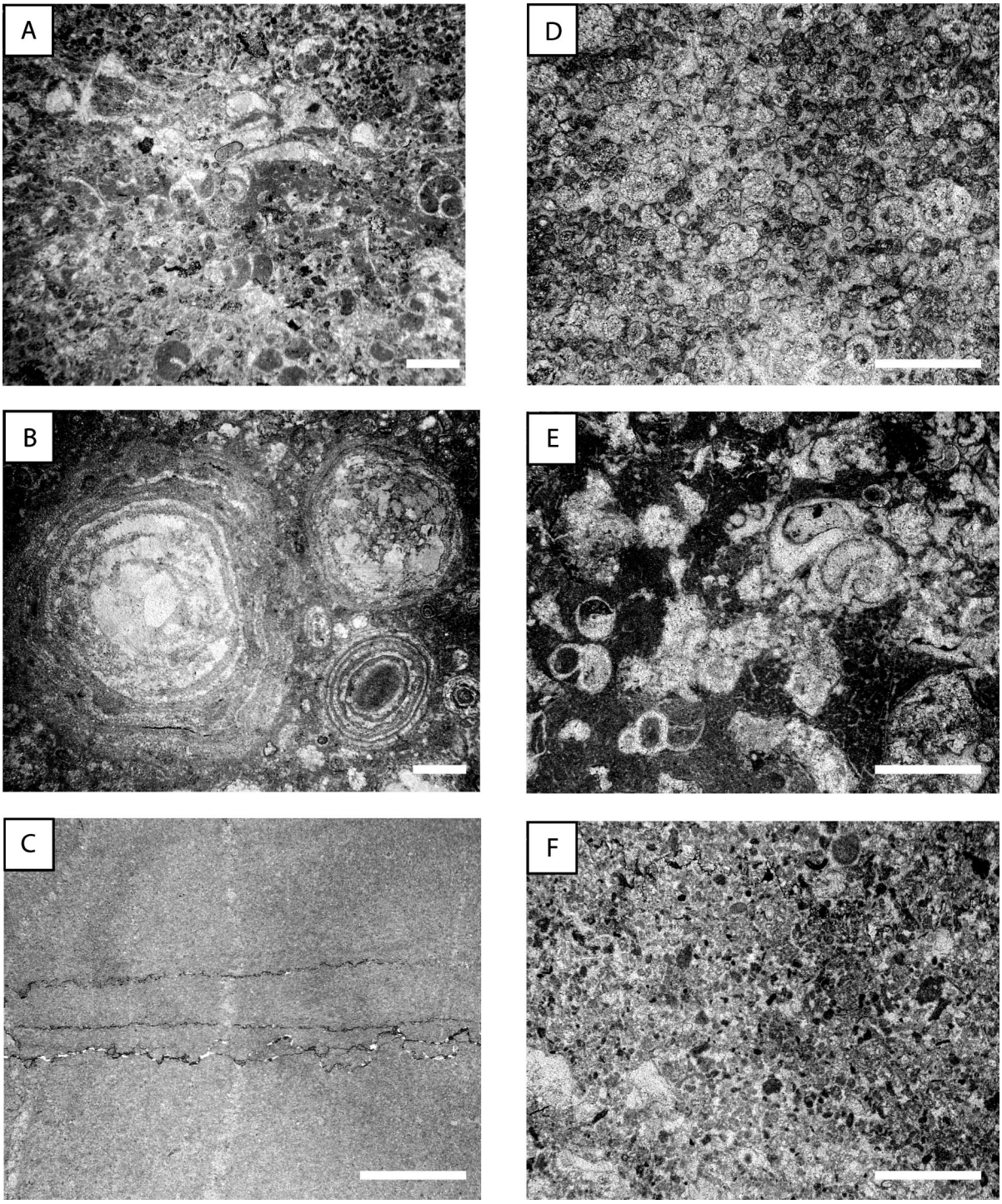

FIGURE 5—Photomicrographs of representative Dienerian and Smithian samples. Scale bars = 2 mm. (A) Dienerian skeletal packstone containing small gastropods and peloidal micrite from the platform margin, Dajiang section (PDJ-221). (B) Oolitic clast illustrating the large size of recrystallized ooids from a Dienerian allodapic breccia exposed in the platform margin, Guandao section (PGD-78). (C) Unfossiliferous Dienerian carbonate mudstone with bedding-parallel stylolites from the basin margin, Guandao section (PGD-52). (D) Recrystallized oolite from the Smithian platform interior (PDJ-310). (E) Smithian skeletal packstone containing small gastropods, Dawen section (PDW-344). (F) Unfossiliferous Smithian peloidal packstone from the Guandao section (PGD-93) on the basin margin.

Ladinian–Carnian

Ladinian and Carnian samples from the Upper Guandao section exhibit little change in abundance and composition of skeletal material relative to the Anisian (online Appendix; Table 7; Fig. 10A–C). The skeletal content remained stable around 8%, well above Lower Triassic levels. *Tubiphytes*, echinoderms, and bivalves dominated the biota, with minor contributions from brachiopods, ostracodes, gastropods, foraminifera, dasyclad algae, and scler-

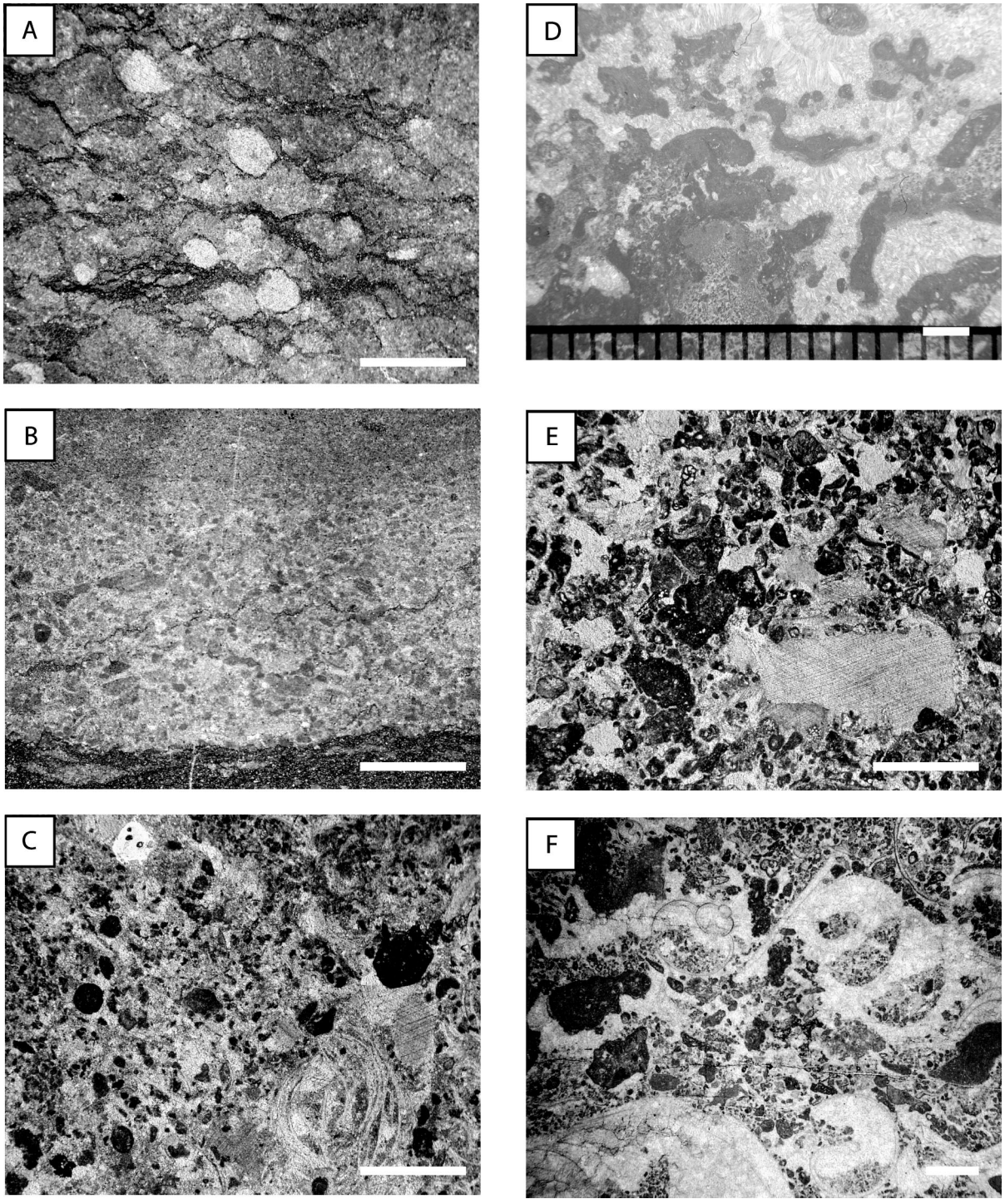

FIGURE 6—Photomicrographs of representative Spathian and Anisian samples. Scale bars = 2 mm. (A) Spathian breccia with small micritic clasts and crinoid ossicles (note clast boundaries are stylolitized) from the platform-margin Guandao section (PGD-152). (B) Unfossiliferous Spathian grainstone exhibiting graded bedding from the Guandao section (PGD-154) on the basin margin. (C) Spathian skeletal grainstone containing crinoid ossicles, dark colored micritic clasts (possibly *Tubiphytes*), and molluscan shell fragments, Guandao section (PGD-191). (D) *Tubiphytes* boundstone from the Anisian reef complex on the platform margin, illustrating the irregular *Tubiphytes* framework and the abundance of early-marine radiaxial fibrous cements. (E) Anisian skeletal grainstone containing crinoid ossicles, *Tubiphytes*, and small micritic grains, Upper Guandao section on the basin margin (PUG-71). (F) Anisian skeletal grainstone containing several gastropods, *Tubiphytes*, and a foraminiferan (*Endothyra*), Guandao section on the basin margin (PGD-229).

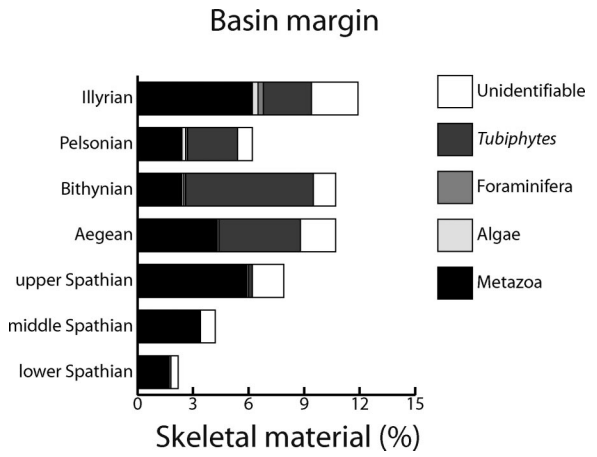

FIGURE 7—Abundance of skeletal material as a fraction of total rock volume for the basin margin from the Spathian to the Anisian. The Spathian samples have been separated informally into three consecutive stratigraphic intervals represented by ten samples each, and the Anisian samples have been subdivided into substages based upon the conodont biostratigraphy.

actinian corals. Middle Triassic samples from the Dajiang section have a very low skeletal content (<1%) dominated by gastropods and bivalves, with minor contributions from echinoderms, foraminifera, ostracodes, and dasyclad algae. These data appear to reflect the continued environmental restriction of the platform interior first established in the Dienerian or Smithian, which was further enhanced by the establishment of the platform-margin reef complex in the Middle Triassic. The apparent lack of recovery in the platform interior suggested by low skeletal abundances is belied by the much larger size of fossils commonly encountered in the field—up to 15 cm.

Summary

Lower Triassic rocks of Griesbachian through Smithian age on the GBG have, in aggregate, very low skeletal content. Gastropods and bivalves are the most abundant skeletal grains across the platform in Griesbachian and Dienerian strata. Smithian samples from the platform margin and basin margin show an increase in the proportion of crinoid grains, but no increase in overall fossil abundance. Skeletal production increased through the Spathian. Spathian strata from the basin margin are dominated by echinoderm debris, especially crinoids, and contain a greater diversity of skeletal material than older Early Triassic rocks. Middle Triassic strata from the basin margin are similar to the Spathian samples in metazoan skeletal content, but also contain large numbers of *Tubiphytes* grains derived from the platform-margin reef complex. Middle Triassic strata also contain much larger crinoids and gastropods than are observed in the Lower Triassic. The shift in community composition and skeletal production appears to have occurred late in the Spathian and early in the Anisian, with relative stability thereafter. The platform interior became a restricted environment during the Dienerian or Smithian, and exhibits low diversity and skeletal content thereafter with gastropods and bivalves as the dominant faunal elements.

DISCUSSION

Carbonate Sedimentation Patterns

The close similarities among Permian–Triassic stratigraphic successions on the Yangtze Platform, the GBG, and the other isolated platforms in the Nanpanjiang Basin (see, e.g., Lehrmann et al., 2003) suggest that the patterns of fossil occurrence and abundance observed on the GBG are representative of a more general pattern within the basin. The other isolated platforms contain the same succession of facies across the Permian–Triassic boundary observed on the GBG, including the development of calcimicrobial precipitates above the extinction horizon and through much or all of the basal Triassic (*Hindeodus parvus* conodont zone; Lehrmann et al., 2003). Both isolated platforms in the Nanpanjiang Basin and the Yangtze Platform also developed marginal-reef complexes in the Anisian supported by a framework of *Tubiphytes* (Lehrmann, 1993; Enos et al., 1997; Lehrmann et al., 2003). More-detailed studies are needed to confirm similar changes in community composition and fossil abundance, but prelim-

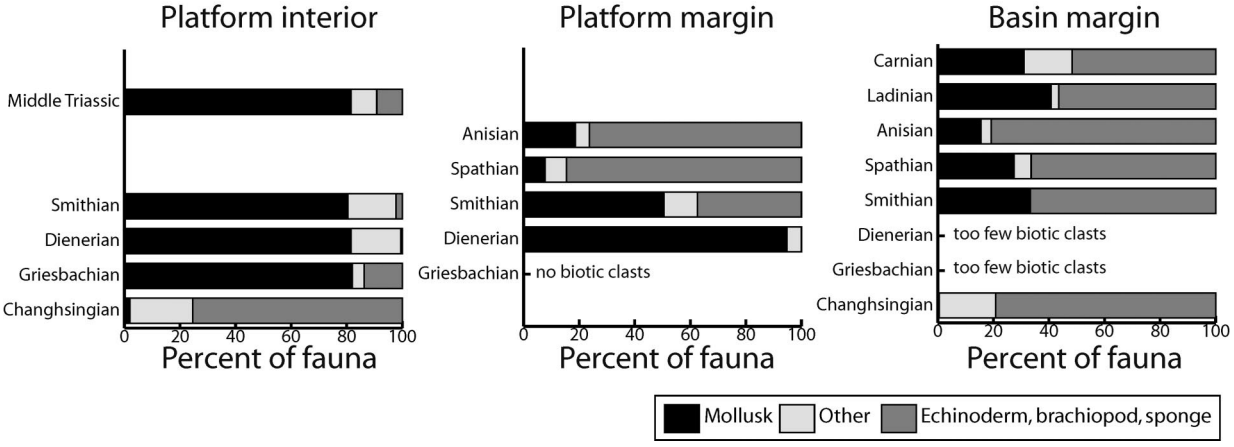

FIGURE 8—Relative abundance of mollusks, non-motile filter feeders (sponges, crinoids, and brachiopods), and other taxa in limestones from the platform interior, platform margin, and basin margin.

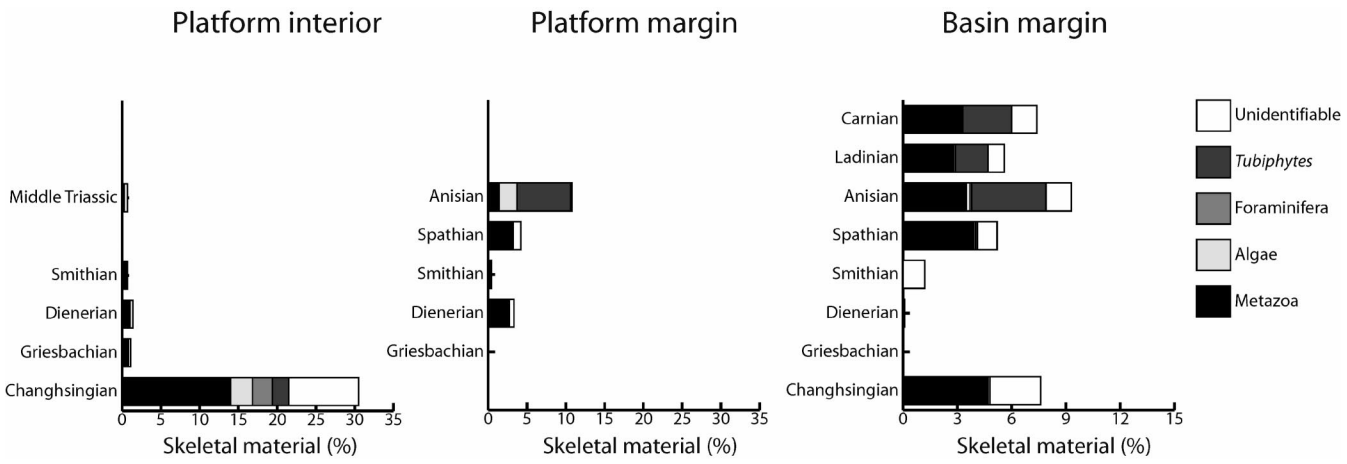

FIGURE 9—Abundance of skeletal material as a fraction of total rock volume for the platform-interior, platform-margin, and basin-margin settings. If a time interval is not listed on the vertical axis in a given environmental setting, no data were collected. Intervals listed but lacking bars have zero or nearly zero skeletal content. Note the different scale used for the platform interior.

inary studies of these other platforms indicate that the GBG is in no way unusual within the basin.

Carbonate strata from more-distant localities indicate that the patterns of skeletal-, calcimicrobial-, and abiotic-carbonate precipitation observed on the GBG are characteristic of deposition across the Tethys and throughout the global tropics from the Permian through the Middle Triassic, especially during the Early Triassic. Quantitative analyses of Middle Permian limestones from the Capitan reef complex (Fagerstrom and Weidlich, 1999) and an Upper Permian reef in Oman (Weidlich et al., 1993), along with published descriptions and photomicrographs of Upper Permian limestones from the Sichuan Basin (Reinhardt, 1988) and Hunan Province (Shen et al., 1998) of China, the Chichibu Terrane (Sano and Nakashima, 1997) and Kitakami Terrane (Kawamura and Machiyama, 1995) of Japan, and the island of Skyros in Greece (Flügel and Reinhardt, 1989), suggest that the contribution of biotic clasts to reefs specifically, and carbonate platforms generally, was substantial—perhaps as high as 10–20% by volume. As on the GBG, calcareous sponges, crinoids, brachiopods, calcareous algae, and foraminifera were among the most abundant biotic clasts. Thus, although Permian reefs, particularly the Capitan reef of Texas and New Mexico, are widely recognized for the prominent role that cements and crusts played in their deposition (e.g., Grotzinger and Knoll, 1995), they also contain a significant fraction of skeletal carbonate.

Carbonate deposition during the earliest Triassic is remarkable because all well-characterized, shallow-water tropical carbonate sections record calcimicrobialites (Baud et al., 1997; Sano and Nakashima, 1997; Kershaw et al., 1999; Lehrmann, 1999; Kershaw et al., 2002; Lehrmann et al., 2003), oolites (Groves and Calner, 2004), or aragonite fans (Heydari et al., 2003). The dominance of bivalve and gastropod grains in Griesbachian through Smithian strata and the increase in the abundance of crinoids in the Spathian observed on the GBG are in accord with studies of relative abundance of individuals from Early Triassic strata elsewhere (Schubert and Bottjer, 1995; Fraiser and Bottjer, 2004). A monograph consisting of photomicrographs of samples from the Spathian Virgin Limestone Member of the Moenkopi Formation in Utah (Bissell, 1970) confirms the high abundance of crinoid debris in those Spathian strata. Taxonomic and lithological descriptions of Early Triassic faunal assemblages from Oman (Twitchett et al., 2004) and Japan (Sano and Nakashima, 1997) also indicate wholesale dominance of Lower Triassic shell beds by mollusks, with additional, small crinoid ossicles. A Spathian increase in crinoid abundance also is observed across Slovenia (Ramovš, 1996). No quantitative data currently are available from localities, apart from the GBG, to compare the volumetric contribution of fossil grains to the accumulation of carbonate sediment.

Although the increase in skeletal content and diversity of platform-margin and basin-margin limestones reflects Middle Triassic recovery, skeletal content on the GBG did not rebound to Late Permian values. The abundance and composition of fossil grains on Middle Triassic carbonate platforms from the Dolomites demonstrate that the GBG likely is representative of this time interval as well. Blendinger (1994) performed point counts on samples from the Marmolada Platform and found that *Tubiphytes* and algae consistently make up approximately 10% of sediment volume and animal skeletal material 3–7%. His use of the grain-bulk method renders these figures as maximum values. However, for many fossil grains (i.e., those lacking internal voids), the grain-bulk and grain-solid methods are equivalent. Therefore, his results suggest a skeletal component very similar to that on the GBG—one dominated by *Tubiphytes*, calcareous sponges, corals, crinoids, and mollusks. Likewise, Keim and Schlager's (2001) volumetric analysis of the Sella Massif in the Dolomites reveals a similar biotic contribution to platform accumulation; fossil grains are less abundant in the platform interior (2.8%) and more abundant on the upper and lower slope (4.7% and 10.8%, respectively). They did not distinguish among types of skeletal material in their tables, but list echinoderms, bivalves, and *Tubiphytes* as the most common skeletal elements. Russo et al. (1997) likewise estimated skeletal contents of 5% and 6% for the Marmolada and Sasso Piatto buildups, respectively, based upon point-counts of platform samples and breccia blocks derived from the platform margin. These data indicate that the GBG is typical

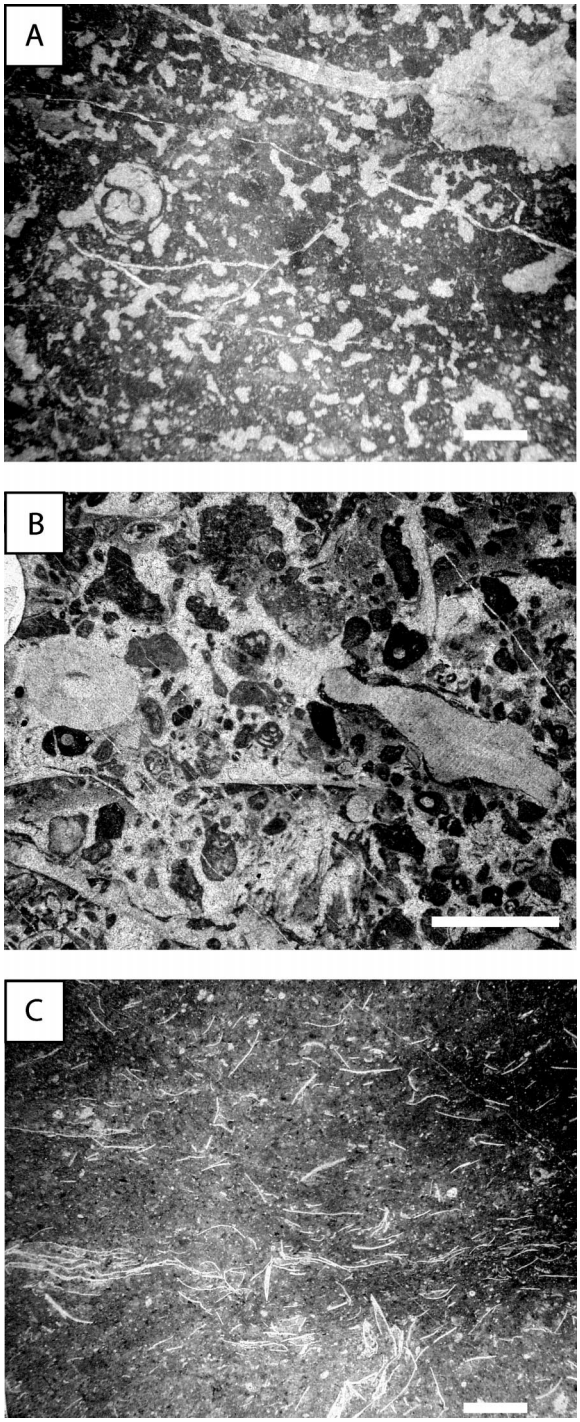

FIGURE 10—Photomicrographs of representative Ladinian and Carnian samples. Scale bars = 2 mm. (A) Middle Triassic fenestral wackestone containing a small gastropod from the platform interior (MDJ-79). (B) Ladinian skeletal grainstone containing an echinoid spine, *Tubiphytes*, and foraminifera, Upper Guandao section on the basin margin (PUG-139). (C) Ladinian pelagic carbonate wackestone containing abundant fragments of thin-shelled bivalves from the basin margin (PUG-103).

of Middle Triassic carbonate platforms across the Tethys in both the abundance and composition of skeletal grains.

The decreased role of organisms in precipitating calcium carbonate under direct enzymatic control may account, at least in part, for the radical change in style of carbonate deposition in the Early Triassic. Specifically, without a significant skeletal sink for calcium carbonate in shallow, shelf settings, deposition would have reverted to predominantly abiotic or microbially mediated forms of precipitation that require higher levels of calcium carbonate saturation than skeletal biomineralization (Riding, 2000). Lower Triassic carbonate rocks have an unusual abundance of microbialites, ooids, and aragonite fans, especially immediately above the end-Permian extinction horizon (e.g., Schubert and Bottjer, 1992; Baud et al., 1997; Lehrmann et al., 2001; Kershaw et al., 2002; Heydari et al., 2003; Lehrmann et al., 2003; Groves and Calner, 2004; Pruss and Bottjer, 2004b). These carbonate fabrics and other sedimentary features, such as the preservation of microbial mat wrinkle structures in siliciclastic settings and the occurrence of ribbon rock and flat-pebble conglomerates in carbonate settings, have been recognized widely as being more characteristic of Proterozoic and Cambrian rocks than subsequent Phanerozoic deposits (Wignall and Twitchett, 1999; Lehrmann et al., 2001; Pruss et al., 2004).

The similarity of carbonate deposition between the Lower Triassic and the Proterozoic is not confined to presence of carbonate fabrics that are otherwise uncommon in Phanerozoic strata. The Lower Triassic stratigraphy of the GBG exhibits proportional thicknesses of lithofacies strikingly reminiscent of those observed in the Neoproterozoic Akademikerbreen Group of Spitsbergen. Knoll and Swett (1990) tabulated the relative thicknesses of micritic limestones, microbialites, and oolites in the ~2000-m-thick Akademikerbreen Group and found ~60% micrites and micrite-derived grainstones, 25% microbialites, and 15% oolites. The resemblance of these proportions to those observed in the Dawen and Dajiang sections of the GBG, particularly for the Griesbachian and Dienerian (Table 2), suggests that carbonate deposition remained in a mode broadly characteristic of the later Proterozoic for an extended interval following the end-Permian extinction. On the other hand, macroscopic seafloor precipitates observed just above the Permian–Triassic boundary in Iran (Heydari et al., 2003), Turkey (Baud et al., 1997), and China (Kershaw et al., 2002) find close parallels in the Neoproterozoic only in postglacial cap carbonates (e.g., Hoffman and Schrag, 2002) and a few other horizons. These features suggest an environmental influence on carbonate deposition beyond the dearth of skeletons. A more comprehensive comparison is necessary to determine how general and meaningful these similarities are.

Even many Middle Triassic platforms have an abundance of problematic, microbial, and abiotic precipitates (e.g., *Tubiphytes*, automicrite, and early marine cements) and a relatively low abundance of the metazoan and algal skeletal materials that characterize most post-Cambrian carbonate platforms (Flügel, 2002). Although diversification occurred throughout the Middle Triassic, it may not have been until later that heavily calcified animals and algae became sufficiently important sinks for calcium carbonate to reduce the relative importance of microbial- and

abiotic-carbonate precipitation. The decreased abundance of marine cements in Late Carnian and Norian–Rhaetian reefs, and the associated rise in the diversity and abundance of large reef-building organisms (Flügel, 2002), may record just such a transition.

Animal Abundance

Overall, the fraction of rock volume consisting of animal-fossil clasts decreased by more than an order of magnitude across the Permian–Triassic boundary in both platform and basin-margin settings (Tables 5, 7; Fig. 9), suggesting a possible decrease in the abundance of skeletal animals. Low animal abundance has been proposed to account for the many taxa that are known to have persisted through the Early Triassic, but have never been observed within these strata (Wignall and Benton, 1999), and for the small size of Early Triassic animals (Twitchett, 2001). Indeed, Lower Triassic strata around the world—particularly beds immediately overlying the extinction horizon—are characterized by reduced fossil abundance and low levels of bioturbation, in settings from tropical carbonate ramps (Twitchett, 1999) to high-latitude siliciclastic deposits (Twitchett et al., 2001). The occurrence of sea-floor aragonite fans (Heydari et al., 2003; Woods et al., 1999), precipitated microbial mounds (Schubert and Bottjer, 1992; Baud et al., 1997), and abundant ooids (Groves and Calner, 2004), along with the global rarity of thick and extensive shell beds (Boyer et al., 2004), provide sedimentological support for a low-abundance scenario.

The absolute abundance of skeletal clasts in any particular stratigraphic section, of course, is affected (and may be controlled) by factors other than the abundance of organisms. Sedimentation rate, sedimentary environment, the rate of post-mortem shell destruction, and the proportion of animals producing mineralized shells can affect the abundance of skeletal material in sediments. In the case of the GBG, however, local changes in sedimentary environment are unlikely to account for the decrease in skeletal content because, aside from a gradual increase in platform relief through the Triassic, the same shallow-marine environments are represented throughout the study interval (Lehrmann et al., 1998). The preservation of the platform-to-basin transition also limits the likelihood that abundant fossils could escape sampling, because, if, as might be expected, they existed near the platform margin, some material transported from this setting would be preserved on the basin margin. Whereas the continued low skeletal abundance in the platform interior during the Middle Triassic is attributable to the development of a platform-margin reef complex during the Anisian that restricted water flow through the platform interior, the low abundance of fossil grains in all environments from the Griesbachian through the Smithian suggests a control beyond the local depositional setting.

The background sedimentation rate (of non-skeletal material) would have needed to increase by a factor of ten to account for the decrease in skeletal content seen in the platform limestones across the Permian–Triassic boundary. There is no indication of such an increase at this time. Backstripping analysis of the Nanpanjiang Basin (Koenig et al., 2001) and calculation of average sedimentation rates from the thicknesses of stratigraphic sections on the GBG, constrained by biostratigraphy and radiometric ages (Mundil et al., 1996; Bowring et al., 1998; Martin et al., 2001; Mundil et al., 2004; Muttoni et al., 2004b; Payne et al., 2004), indicate that average sediment-accumulation rate at the stage level did not vary by more than a factor of two or three—much less than observed changes in fossil abundance.

Although the small, aragonitic shells of bivalves and gastropods may have been more susceptible to post-mortem destruction than larger, calcitic Permian shells, the abundance of precipitated, originally aragonitic thrombolites, ooids, and marine cements deposited directly on Early Triassic shells suggests rates of dissolution decreased, if they changed at all, in the Early Triassic. A concern might be that much of the micrite in Lower Triassic strata is derived from comminuted remains of animal shells. However, animal shells are not the primary source of micrite on modern carbonate platforms, and could not have been the source of micrite on extensive Precambrian carbonate platforms. Furthermore, rates of shell crushing (Oji et al., 2003) and shell-drilling predation (Kowalewski et al., 1998) apparently were low during the Early Triassic. The magnitude of the decrease in skeletal abundance is difficult to account for by the onset of more intense physical or biological erosion of shells in the Early Triassic, particularly given evidence for reduced rates of biological shell destruction and high rates of early marine carbonate precipitation.

The low overall abundance of fossil grains on the GBG is most consistent with decreased abundance of skeletal animals. If so, the long duration of low skeletal abundance (~3 Ma) precludes any explanation based upon the immediate effects of the end-Permian mass extinction. Even extremely low rates of population growth, such as 0.1% per year, would result in full repopulation in much less than 100 ky. The persistently low skeletal content of GBG carbonates from the Griesbachian through the Smithian must reflect persistently low rates of skeletal production.

One implication of this interpretation is that the proportional dominance of mollusks in the Early Triassic benthic community on the GBG may be at least as much a consequence of the removal of the rest of the fauna as it is an opportunistic response to the end-Permian mass extinction. The proportional dominance of mollusks in Lower Triassic rocks has been interpreted as an opportunistic response to Early Triassic environmental and ecological conditions (Schubert and Bottjer, 1995; Krystyn et al., 2003; Fraiser and Bottjer, 2004). Although mollusks were the only group to increase in absolute abundance on the GBG across the Permian–Triassic boundary, their abundance as a fraction of rock volume did not increase substantially. In fact, only within the platform interior did bivalves and gastropods increase in abundance as a proportion of rock volume. From the Changhsingian to the Griesbachian, bivalves increased from 0.07% of total rock volume to 0.33% of rock volume. Gastropods increased from 0.25% to 0.29% of rock volume—a change that can hardly be viewed as significant. Although bivalves are the most abundant fossil grains in the Griesbachian platform interior, their shells are less abundant than those of sponges, crinoids, brachiopods, bryozoans, dasyclad algae, foraminifera, or *Tubiphytes* in the Changhsingian. Thus, despite the fact that bivalves were the dominant component of Early Triassic as-

semblages locally, their proportional increase in abundance did not necessarily translate into a significant increase in standing biomass. This is not to say that bivalves and gastropods were unaffected by the extinction. On the contrary, both experienced substantial extinction, and the most abundant genera of bivalves and gastropods in the Early Triassic were not necessarily similarly abundant in the Late Permian (Hallam and Wignall, 1997). Rather, bivalves and gastropods appear to have increased in total abundance only slightly, if at all, even if individual genera increased substantially. Individual shell beds could represent local, short-term population booms, at the same time that the low overall abundance of skeletal material within entire sections reflects a low mean abundance of organisms averaged over hundreds of thousands of years. On the other hand, such a scenario is difficult to distinguish from the concentration of shells by purely sedimentary processes.

In principle, increased abundance of soft-bodied animals could have compensated for decreased abundance of skeletonized animals. Inferring the abundance of the nonskeletonized fauna in ancient communities is difficult, but intensity of bioturbation and the distribution of burrow sizes can serve as independent indicators of non-mineralized animal biomass in marine benthic communities, at least for motile organisms. Trace fossils are small and limited in distribution in Lower Triassic strata in both low- and high-latitude settings (Pruss and Bottjer, 2004a; Twitchett, 1999; Twitchett et al., 2001), suggesting that motile, soft-bodied animals decreased in abundance in parallel with the animals with hard shells, rather than increasing in response to potentially decreased competition. The preservation of wrinkle structures from microbial mats in open-marine settings further reflects low intensity of grazing and bioturbation (Pruss et al., 2004). The abundance of non-motile, non-mineralized organisms, such as sponges and cnidarians, is more challenging to assess; however, the extensive preservation of microbialites in lowest Triassic carbonates across southern China (Lehrmann et al., 2003) and elsewhere (Baud et al., 1997; Sano and Nakashima, 1997) and the widespread occurrence of microbial fabrics in siliciclastic beds (Pruss et al., 2004) suggest that even benthic, non-motile animals could not have lived in high density over much of the shallow seafloor, at least not in the immediate aftermath of the extinction event. Sterol biomarkers for sponges, recovered in relative abundance from Neoproterozoic and Cambrian strata, are not found in significant concentrations within Lower Triassic deposits (McCaffrey et al., 1994). If soft-bodied animals did increase in abundance during the Early Triassic, they were most likely pelagic forms.

Reduced animal biomass through the Early Triassic could result from two different processes—a decrease in food availability or a decrease in the efficiency with which available food was converted into animal biomass. There are no direct geological proxies for Early Triassic primary productivity; contrary to a low-productivity scenario (Twitchett, 2001), however, modeling suggests that evidence for widespread anoxia in Early Triassic oceans (Wignall and Twitchett, 2002) likely reflects, and may require, high rates of primary production (Hotinski et al., 2001). In contrast, three lines of evidence indicate that the mean metabolic rates of marine benthic invertebrates increased from the Permian to the Early Triassic, a factor that would decrease animal growth efficiency. Mollusks dominate Early Triassic fossil assemblages (Tables 5–7; Boyer et al., 2004; Fraiser and Bottjer, 2004; Schubert and Bottjer, 1995), and these animals had much higher specific (i.e., per gram) metabolic rates than dominant Permian taxa such as sponges, brachiopods, and crinoids (Bambach, 1993). Metabolic rates tend to scale inversely with size (Schmidt-Nielsen, 1984); therefore, the generally small size of the Early Triassic fauna (Twitchett, 2001; Fraiser and Bottjer, 2004; Payne, 2005) also should carry with it an increase in the mean per-gram metabolic rate. Additionally, metabolic rates in organisms from bacteria to animals scale strongly with temperature—the so-called Q_{10} effect, long recognized by physiologists (Cossins and Bowler, 1987); therefore, greenhouse conditions established across the Permian–Triassic boundary (Retallack, 1999) would have tended to increase metabolic rates in all organisms. On average, then, Early Triassic animals may have had large energenic demand per gram of tissue relative to their Permian counterparts.

Previous hypotheses for end-Permian catastrophe include the physiological consequences of sharply elevated P_{CO2} (Knoll et al., 1996), which correctly predicts observed patterns of extinction in the oceans. Elevated CO_2 levels are indicated by low stomatal densities on the leaves of Early Triassic plants (Retallack, 2001; Retallack, 2002) and may, in fact, be required to explain evidence for extreme warming at this time (Retallack, 1999). Unfortunately, long-term, geochemical proxy models for atmospheric CO_2 concentrations (e.g., Berner and Kothavala, 2001; Ekart et al., 1999) have insufficient resolution to track changes in atmospheric CO_2 through the Early Triassic and, in some cases (e.g., Ekart et al., 1999), are not constrained by any data from Lower Triassic samples. Mechanisms potentially responsible for an intermittent or sustained Early Triassic greenhouse climate and elevated P_{CO2} are poorly understood. Siberian Traps eruptions, in part through interactions with crustal carbonate rocks and organic deposits, are one potential source of CO_2. However, the bulk of Traps eruptions appear to be contained to a rather brief interval near the Permian–Triassic boundary (Kamo et al., 2003). The size of the methane clathrate reservoir, the long timescale for clathrate generation, and the short lifetime of methane in the atmosphere argue against a role for methane clathrates in a sustained greenhouse climate.

Not previously explored in detail are the interactive effects of high temperature and physiology. Rates of photosynthesis are fundamentally limited by nutrient availability, so increased temperature would be unlikely to enhance primary productivity. In contrast, the proposed sharp increase in global temperatures should have decreased the growth efficiency and biomass of bacterial heterotrophs that are a primary food source for filter-feeding animals and detritivores (see, e.g., Fang et al., 2005). In conjunction with this decrease in available bacterial biomass, concomitantly increasing metabolic rates of the animals themselves could account for the substantial decrease in animal biomass inferred for Early Triassic oceans.

Interactions between temperature and physiology may explain other Early Triassic phenomena as well. The abil-

ity of the respiratory system to meet increased oxygen demands at higher temperatures limits thermal tolerance in many animal taxa (Cossins and Bowler, 1987). Temperatures higher than 45°C may present a fundamental limit to metazoan biology, although the precise upper limit for long-term viability varies between taxa and depends, in part, upon the design and efficiency of the respiratory system (Cossins and Bowler, 1987). High temperatures could have limited the recovery of clades with less-adaptable respiratory systems (e.g., sponges, cnidarians, echinoderms, brachiopods) by pushing cellular oxygen demand beyond the capacity of their respiratory systems, an effect exacerbated to varying degrees by the direct effects of CO_2 on the capacity of respiratory pigments to carry oxygen (the Bohr effect; Jensen, 2004). Greenhouse conditions also would decrease oxygen solubility (Hotinski et al., 2001), explaining geological evidence for widespread anoxia at this time (Wignall and Twitchett, 2002), which would have provided an additional respiratory stress on marine animals. A combination of high temperatures, high P_{CO2}, and low oxygen concentrations may help to explain the dominance of mollusks in nearly all Early Triassic marine communities, particularly at low paleolatitudes (Fraiser and Bottjer, 2004; Schubert and Bottjer, 1995; Twitchett et al., 2004). Evidence for more rapid recovery in high-latitude settings (e.g., Zonneveld et al., 2002), and the occurrence of tropical Permian taxa at high paleolatitudes in Lower Triassic rocks (e.g., Retallack, 2002) also are consistent with this scenario. Increased rates of microbial respiration at high temperatures may account for the absence of coal (Retallack et al., 1996) in Lower Triassic terrestrial strata.

Pattern and Timing of Global Biotic Recovery

Studies of the Triassic recovery interval have provided data on several independent metrics of recovery, such as global biodiversity (Erwin, 1993), diversity and relative abundance of taxa in local communities (Schubert and Bottjer, 1995; Rodland and Bottjer, 2001; Boyer et al., 2004; Twitchett et al., 2004), the size distribution of organisms regionally (Fraiser and Bottjer, 2004) and globally (Payne, 2005), patterns of sedimentation (e.g., Baud et al., 1997; Lehrmann et al., 2003; Pruss, 2004), and the abundance of animals in marine communities (this study). Each of these metrics indicates that measurable recovery did not begin until the Spathian at the earliest, confirming in much greater detail the long-recognized delay of biotic recovery until the Middle Triassic (e.g., Stanley, 1988; Stanley, 1990; Hallam, 1991).

A major remaining issue is the degree to which recovery during the Early Triassic was gradational or geographically heterogeneous. This question is particularly challenging because at finer spatial and temporal resolutions, local artifacts of environment, sampling strategy, and taphonomy are more likely to influence the local recovery pattern. These types of influences are apparent on the GBG in the differences in proportional abundance of mollusks and crinoids between the platform interior and the basin margin during the Early Triassic, and the differences in fossil occurrence and abundance patterns among different lithofacies in the platform interior. Taken as a whole, however, the biota on the GBG appears stable at the substage level, especially from the Griesbachian through the Smithian.

Recently, Twitchett et al. (2004) proposed a four-stage model of recovery from the end-Permian extinction, and suggested that the pace of recovery differed among localities. The primary distinction among the first three stages of recovery in their model is local diversity, with stages one through three characterized by 0–5, 5–10, and 10 or more taxa, respectively. They argued that the relatively diverse fauna found in a Griesbachian to Dienerian shallow-water carbonate section from Oman represents locally accelerated recovery in the absence of anoxic conditions more prevalent in other areas. The heterogeneity of fossil content among individual beds and lithofacies on the GBG that, in aggregate, actually represent a stable set of organisms throughout the Early Triassic suggests that Twitchett et al.'s (2004) interpretation of their data using their four-stage recovery model may confuse facies-related controls on local diversity with ecological and evolutionary controls on global recovery. On the GBG, at least nine metazoan taxa are distinguishable in thin section for all substages of the Early Triassic (online Appendix). Preservation adequate for genus-level classification almost certainly would lead to the identification of more than ten genera in all cases. Second, identifiable crinoid ossicles occur in all substages except the Dienerian on the GBG. This observation is not a surprise, given that crinoids survived the end-Permian extinction, but it highlights the fact that the minimal epifaunal tiering that Twitchett et al. (2004) attributed to their third stage of recovery likely existed throughout the Early Triassic. Even if purported increases in the diversity and ecological structure of communities through the Early Triassic are not merely the results of local environmental controls, the stark differences in size, abundance, and composition of skeletal grains on the GBG and elsewhere between the earlier Triassic and the Spathian–Anisian recovery interval emphasize that the Middle Triassic recovery far exceeds any recovery observed within Lower Triassic strata.

CONCLUSIONS

Analysis of skeletal abundance of major invertebrate and algal groups on the Great Bank of Guizhou, from the Late Permian through Middle Triassic, demonstrates that it is possible both to determine the proportional contribution of various taxa to platform accumulation, and to track changes in fossil abundance, diversity, and composition across an environmental gradient from the platform interior to the basin margin. A decrease in fossil diversity and abundance across the Permian–Triassic boundary is observed at all scales, from individual thin sections to the entire carbonate platform. The Late Permian fauna was dominated by calcareous sponges, crinoids, and brachiopods, and included many subordinate taxa. Early and Middle Triassic communities on the GBG, even in the immediate aftermath of the extinction, were dominated by small mollusks, with increasing abundance of crinoids beginning in the Spathian. On the GBG, the primary increase in diversity and abundance was confined to a brief interval late in the Spathian and early in the Anisian, and was concentrated primarily along the platform margin. Middle Triassic diversification, the return of calcareous al-

gae, and the appearance of scleractinian corals are observed on the GBG, but they do not substantially alter the pattern established at the base of the Anisian of a biota dominated by mollusks, crinoids, and *Tubiphytes*.

The low abundance of skeletal grains in Lower Triassic strata can help to explain several phenomena. The abundance of micrite, microbialites, and large ooids, similar to Neoproterozoic carbonates, results from the removal of the skeletal sink for calcium carbonate, and may reflect a return of oceanic carbonate chemistry to conditions that had not been widely experienced for nearly 300 million years. Animals with hard skeletons remained at low abundance from the time of the end-Permian extinction through much of the Early Triassic. Therefore, the high proportional abundance of bivalves and gastropods in Lower Triassic strata is as much a consequence of the removal of other sources of biotic skeletal material as an opportunistic response to the empty Early Triassic ecosystems. Geographically widespread data on the absolute abundance of fossil grains generally, and mollusks in particular, from Upper Permian and Lower and Middle Triassic strata should provide new insights that will better constrain the ecological processes underlying the recovery of biotic diversity and abundance following the greatest crisis in the history of animal life.

Fossil-abundance data from the GBG demonstrate the possibility of tracking both the relative and absolute abundance of fossil grains through the entire recovery interval following the end-Permian mass extinction. Such data not only may enrich understanding of the ecological and evolutionary processes governing biotic recovery from the end-Permian mass extinction, but also provide a new avenue of progress in tracing changes in the abundance and composition of the biota in marine benthic communities through Phanerozoic time.

ACKNOWLEDGEMENTS

We thank Y. Yu, J. Xiao, H. Yao, H. Wang, A. Bush, and R. Kodner for assistance in the field. R. Bambach, W. Fischer, C. Marshall, and S. Pruss were sources of helpful discussion and provided insightful comments on the manuscript. We are grateful to S. Kershaw and P. Wignall for helpful and thoughtful reviews. This work was funded by the National Science Foundation (Grants OCE-0084032 to AHK—Project EREUPT, and EAR-9804835 to DJL), the Petroleum Research Fund of the American Chemical Society (Grant 40948-B2 to DJL), Sigma Xi (Grant-in-aid of Research to JLP), and the Department of Defense (National Defense Science and Engineering Graduate Fellowship to JLP).

REFERENCES

ATUDOREI, N.-V., 1999, Constraints on the Upper Permian to Upper Triassic marine carbon isotope curve. Case studies from the Tethys: Unpublished PhD dissertation, University of Lausanne, Lausanne, 160 p.

ATUDOREI, V., and BAUD, A., 1997, Carbon isotope events during the Triassic: Albertiana, v. 20, p. 45–49.

BAMBACH, R.K., 1993, Seafood through time—changes in biomass, energetics, and productivity in the marine ecosystem: Paleobiology, v. 19, p. 372–397.

BAMBACH, R.K., KNOLL, A.H., and SEPKOSKI, J.J., JR., 2002, Anatomical and ecological constraints on Phanerozoic animal diversity in the marine realm: Proceedings of the National Academy of Sciences of the United States of America, v. 99, p. 6854–6859.

BASU, A.R., PETAEV, M.I., POREDA, R.J., JACOBSEN, S.B., and BECKER, L., 2003, Chondritic meteorite fragments associated with the Permian–Triassic boundary in Antarctica: Science, v. 302, p. 1388–1392.

BATTEN, R.L., 1973, The vicissitudes of the Gastropoda during the interval of Guadalupian–Ladinian time: *in* Logan, A., and Hills, L.V., eds., The Permian and Triassic Systems and Their Mutual Boundary: Canadian Society of Petroleum Geologists, Calgary, p. 596–607.

BAUD, A., ATUDOREI, V., and SHARP, Z., 1996, Late Permian and early Triassic evolution of the Northern Indian margin: carbon isotope and sequence stratigraphy: Geodinamica Acta, v. 9, p. 57–77.

BAUD, A., BRANDNER, R., and DONOFRIO, D.A., 1991, The Sefid Kuh limestone—a late Lower Triassic carbonate ramp (Aghdarband, NE-Iran): Abhandlungen der Geologisches Bundesanstalt, v. 38, p. 111–123.

BAUD, A., CIRILLI, S., and MARCOUX, J., 1997, Biotic response to mass extinction: the lowermost Triassic microbialites: Facies, v. 36, p. 238–242.

BECKER, L., POREDA, R.J., BASU, A.R., POPE, K.O., HARRISON, T.M., NICHOLSON, C., and IASKY, R., 2004, Bedout: a possible end-Permian impact crater offshore of Northwestern Australia: Science, v. 304, p. 1469–1476.

BECKER, L., POREDA, R.J., HUNT, A.G., BUNCH, T.E., and RAMPINO, M., 2001, Impact event at the Permian–Triassic boundary: evidence from extraterrestrial noble gases in fullerenes: Science, v. 291, p. 1530–1533.

BERNER, R.A., and KOTHAVALA, Z., 2001, GEOCARB III: a revised model of atmospheric CO_2 over Phanerozoic time: American Journal of Science, v. 301, p. 182–204.

BISSELL, H.J., 1970, Petrology and Petrography of Lower Triassic Marine Carbonates of Southern Nevada (U.S.A.): E. J. Brill, Leiden, 111 p.

BLENDINGER, W., 1994, The carbonate factory of Middle Triassic buildups in the Dolomites, Italy—a quantitative analysis: Sedimentology, v. 41, p. 1147–1159.

BOWRING, S.A., ERWIN, D.H., JIN, Y.G., MARTIN, M.W., DAVIDEK, K., and WANG, W., 1998, U/Pb zircon geochronology and tempo of the end-Permian mass extinction: Science, v. 280, p. 1039–1045.

BOYER, D.L., BOTTJER, D.J., and DROSER, M.L., 2004, Ecological signature of Lower Triassic shell beds of the western United States: PALAIOS, v. 19, p. 372–380.

COSSINS, A.S., and BOWLER, K., 1987, Temperature Biology of Animals: Chapman and Hall, New York, 337 p.

EKART, D.D., CERLING, T.E., MONTANEZ, I.P., and TABOR, N.J., 1999, A 400 million year carbon isotope record of pedogenic carbonate: implications for paleoatmospheric carbon dioxide: American Journal of Science, v. 299, p. 805–827.

ENOS, P., WEI, J.Y., and YAN, Y.J., 1997, Facies distribution and retreat of Middle Triassic platform margin, Guizhou Province, South China: Sedimentology, v. 44, p. 563–584.

ERWIN, D.H., 1993, The Great Paleozoic Crisis: Life and Death in the Permian: Columbia University Press, New York, 327 p.

ERWIN, D.H., 1996, Understanding biotic recoveries: extinction, survival, and preservation during end-Permian mass extinction: *in* Erwin, D.H., Jablonski, D., and Lipps, J.H., eds., Evolutionary Paleobiology: University of Chicago Press, Chicago, p. 398–418.

ERWIN, D.H., 1998, The end and the beginning: recoveries from mass extinctions: Trends in Ecology and Evolution, v. 13, p. 344–349.

ERWIN, D.H., SOLE, R.V., and MONTOYA, J.M., 2004, Models of recovery dynamics following mass extinction: Geological Society of America Abstracts with Programs, v. 36, p. 335.

FAGERSTROM, J.A., and WEIDLICH, O., 1999, Strengths and weaknesses of the Reef Guild concept and quantitative data: application to the upper Capitan massive community (Permian), Guadalupe Mountains, New Mexico Texas: Facies, v. 40, p. 131–156.

FANG, C., SMITH, P., MONCRIEFF, J.B., and SMITH, J.U., 2005, Similar response of labile and resistant soil organic matter pools to changes in temperature: Nature, v. 433, p. 57–59.

FLÜGEL, E., 1982, Microfacies Analysis of Limestones: Springer, New York, 633 p.
FLÜGEL, E., 1985, Diversity and environments of Permian and Triassic dasycladacean algae: *in* Toomey, D.F., and Nitecki, M.H., eds., Paleoalgology: Contemporary Research and Applications: Springer, Berlin, p. 344–351.
FLÜGEL, E., 1994, Pangean shelf carbonates: controls and paleoclimatic significance of Permian and Triassic reefs: *in* Klein, G.D., ed., Pangea: Paleoclimate, Tectonics, and Sedimentation during Accretion, Zenith, and Breakup of a Supercontinent: Geological Society of America Special Paper 288. p. 247–266.
FLÜGEL, E., 2002, Triassic reef patterns: *in* Kiessling, W., Flügel, E., and Golonka, J., eds., Phanerozoic Reef Patterns: SEPM Special Publication 72, p. 391–464.
FLÜGEL, E., and REINHARDT, J., 1989, Uppermost Permian reefs in Skyros (Greece) and Sichuan (China): implications for the Late Permian extinction event: PALAIOS, v. 4, p. 502–518.
FRAISER, M.L., and BOTTJER, D.J., 2004, The non-actualistic early Triassic gastropod fauna: a case study of the Lower Triassic Sinbad Limestone Member: PALAIOS, v. 19, p. 259–275.
GROTZINGER, J.P., and KNOLL, A.H., 1995, Anomalous carbonate precipitates: is the Precambrian the key to the Permian?: PALAIOS, v. 10, p. 578–596.
GROVES, J.R., and CALNER, M., 2004, Lower Triassic oolites in Tethys: a sedimentologic response to the end-Permian mass extinction: Geological Society of America Abstracts with Programs, v. 36, p. 336.
HALLAM, A., 1991, Why was there a delayed radiation after the end-Paleozoic extinctions?: Historical Biology, v. 5, p. 257–262.
HALLAM, A., and WIGNALL, P.B., 1997, Mass Extinctions and their Aftermaths: Oxford University Press, New York, 320 p.
HEYDARI, E., HASSANZADEH, J., WADE, W.J., and GHAZI, A.M., 2003, Permian–Triassic boundary interval in the Abadeh section of Iran with implications for mass extinction: part 1—sedimentology: Palaeogeography, Palaeoclimatology, Palaeoecology, v. 193, p. 405–423.
HOFFMAN, P.F., and SCHRAG, D.P., 2002, The Snowball Earth hypothesis: testing the limits of global change: Terra Nova, v. 14, p. 129–155.
HORACEK, M., ABART, R., and BRANDNER, R., 2001, Carbon isotope record of the Permo/Triassic boundary and the Lower Triassic: *in* Wanek, W., Richter, A., Wiener, S., and Hood, R., eds., Third Viennese Workshop on Stable Isotopes in Biological and Environmental Sciences: University of Vienna, Vienna, p. 10–11.
HOTINSKI, R.M., BICE, K.L., KUMP, L.R., NAJJAR, R.G., and ARTHUR, M.A., 2001, Ocean stagnation and end-Permian anoxia: Geology, v. 29, p. 7–10.
JAANUSSON, V., 1972, Constituent analysis of an Ordovician limestone from Sweden: Lethaia, v. 5, p. 217–237.
JABLONSKI, D., 1986, Causes and consequences of mass extinctions: a comparative approach: *in* Elliott, D.K., ed., Dynamics of Extinction: John Wiley & Sons, New York, p. 183–229.
JENSEN, F.B., 2004, Red blood cell pH, the Bohr effect, and other oxygenation-linked phenomena in blood O-2 and CO2 transport: Acta Physiologica Scandinavica, v. 182, p. 215–227.
JIN, Y.G., WANG, Y., WANG, W., SHANG, Q.H., CAO, C.Q., and ERWIN, D.H., 2000, Pattern of marine mass extinction near the Permian–Triassic boundary in South China: Science, v. 289, p. 432–436.
KAMO, S.L., CZAMANSKE, G.K., AMELIN, Y., FEDORENKO, V.A., DAVIS, D.W., and TROFIMOV, V.R., 2003, Rapid eruption of Siberian floodvolcanic rocks and evidence for coincidence with the Permian–Triassic boundary and mass extinction at 251 Ma: Earth and Planetary Science Letters, v. 214, p. 75–91.
KAWAMURA, T., and MACHIYAMA, H., 1995, A Late Permian coral-reef complex, South Kitakami Terrane, Japan: Sedimentary Geology, v. 99, p. 135–150.
KEIM, L., and SCHLAGER, W., 2001, Quantitative compositional analysis of a Triassic carbonate platform (Southern Alps, Italy): Sedimentary Geology, v. 139, p. 261–283.
KERSHAW, S., GUO, L., SWIFT, A., and FAN, J.S., 2002, Microbialites in the Permian–Triassic boundary interval in central China: structure, age and distribution: Facies, v. 47, p. 83–89.
KERSHAW, S., ZHANG, T.S., and LAN, G.Z., 1999, A ?microbialite carbonate crust at the Permian–Triassic boundary in South China, and its palaeoenvironmental significance: Palaeogeography, Palaeoclimatology, Palaeoecology, v. 146, p. 1–18.
KIDDER, D.L., and WORSLEY, T.R., 2004, Causes and consequences of extreme Permo–Triassic warming to globally equable climate and relation to the Permo–Triassic extinction and recovery: Palaeogeography, Palaeoclimatology, Palaeoecology, v. 203, p. 207–237.
KNOLL, A.H., BAMBACH, R.K., CANFIELD, D.E., and GROTZINGER, J.P., 1996, Comparative Earth history and Late Permian mass extinction: Science, v. 273, p. 452–457.
KNOLL, A.H., and SWETT, K., 1990, Carbonate deposition during the Late Proterozoic Era—an example from Spitsbergen: American Journal of Science, v. 290A, p. 104–132.
KOBAYASHI, F., 1997, Upper Permian foraminifers from the Iwai-Kanyo area, West Tokyo, Japan: Journal of Foraminiferal Research, v. 27, p. 186–195.
KOENIG, J., DILLETT, P., LEHRMANN, D.J., and ENOS, P., 2001, Structural and paleogeographic elements of the Nanpanjiang Basin, Guizhou, Guangxi, and Yunnan provinces, south China: a compilation from satellite images, regional geologic maps and ground observations: American Association of Petroleum Geologists Official Program, v. 10, p. A107.
KOWALEWSKI, M., DULAI, A., and FÜRSICH, F.T., 1998, A fossil record full of holes: the Phanerozoic history of drilling predation: Geology, v. 26, p. 1091–1094.
KÖYLÜOGLU, M., and ALTINER, D., 1989, Micropaleontologie (Foraminiferes) et biostratigraphie du Permien superieur de la region d'Hakkari (SE Turquie): Revue de Paléobiologie, v. 8, p. 467–503.
KRYSTYN, L., RICHOZ, S., BAUD, A., and TWITCHETT, R.J., 2003, A unique Permian–Triassic boundary section from the Neotethyan Hawasina Basin, Central Oman Mountains: Palaeogeography, Palaeoclimatology, Palaeoecology, v. 191, p. 329–344.
LEHRMANN, D.J., 1993, Sedimentary geology of the Great Bank of Guizhou: birth, evolution and death of a Triassic isolated carbonate platform, Guizhou Province, South China: Unpublished PhD dissertation, University of Kansas, Lawrence, 457 p.
LEHRMANN, D.J., 1999, Early Triassic calcimicrobial mounds and biostromes of the Nanpanjiang Basin, South China: Geology, v. 27, p. 359–362.
LEHRMANN, D.J., PAYNE, J.L., FELIX, S.V., DILLETT, P.M., WANG, H., YU, Y.Y., and WEI, J.Y., 2003, Permian–Triassic boundary sections from shallow-marine carbonate platforms of the Nanpanjiang Basin, south China: implications for oceanic conditions associated with the end-Permian extinction and its aftermath: PALAIOS, v. 18, p. 138–152.
LEHRMANN, D.J., WAN, Y., WEI, J.Y., YU, Y.Y., and XIAO, J.F., 2001, Lower Triassic peritidal cyclic limestone: an example of anachronistic carbonate facies from the Great Bank of Guizhou, Nanpanjiang Basin, Guizhou Province, South China: Palaeogeography, Palaeoclimatology, Palaeoecology, v. 173, p. 103–123.
LEHRMANN, D.J., WEI, J.Y., and ENOS, P., 1998, Controls on facies architecture of a large Triassic carbonate platform: the Great Bank of Guizhou, Nanpanjiang Basin, South China: Journal of Sedimentary Research, v. 68, p. 311–326.
MARENCO, P.J., CORSETTI, F.A., BAUD, A., BOTTJER, D.J., and KAUFMAN, A.J., 2004, Sulfur isotope anomalies across Permo–Triassic boundary sections in Turkey: Geological Society of America Abstracts with Programs, v. 36, p. 335.
MARTIN, M.W., LEHRMANN, D.J., BOWRING, S.A., ENOS, P., RAMEZANI, J., WEI, J.Y., and ZHANG, J., 2001, Timing of Lower Triassic carbonate bank buildup and biotic recovery following the end-Permian extinction across the Nanpanjiang Basin, south China: Geological Society of America Abstracts with Programs, v. 33, p. 201.
MCCAFFREY, M.A., MOLDOWAN, J.M., LIPTON, P.A., SUMMONS, R.E., PETERS, K.E., JEGANATHAN, A., and WATT, D.S., 1994, Paleoenvironmental implications of novel C-30 steranes in Precambrian to Cenozoic age petroleum and bitumen: Geochimica et Cosmochimica Acta, v. 58, p. 529–532.
MCGHEE, G.R., SHEEHAN, P.M., BOTTJER, D.J., and DROSER, M.L., 2004, Ecological ranking of Phanerozoic biodiversity crises: ecological and taxonomic severities are decoupled: Palaeogeography, Palaeoclimatology, Palaeoecology, v. 211, p. 289–297.
MUNDIL, R., BRACK, P., MEIER, M., RIEBER, H., and OBERLI, F., 1996,

High resolution U-Pb dating of Middle Triassic volcaniclastics: time-scale calibration and verification of tuning parameters for carbonate sedimentation: Earth and Planetary Science Letters, v. 141, p. 137–151.

MUNDIL, R., LUDWIG, K.R., METCALFE, I., and RENNE, P.R., 2004, Age and timing of the Permian mass extinctions: U/Pb dating of closed-system zircons: Science, v. 305, p. 1760–1763.

MUTTONI, G., KENT, D.V., OLSEN, P.E., DI STEFANO, P., LOWRIE, W., BERNASCONI, S.M., and HERNANDEZ, F.M., 2004a, Tethyan magnetostratigraphy from Pizzo Mondello (Sicily) and correlation to the Late Triassic Newark astrochronological polarity time scale: Geological Society of America Bulletin, v. 116, p. 1043–1058.

MUTTONI, G., NICORA, A., BRACK, P., and KENT, D.V., 2004b, Integrated Anisian–Ladinian boundary chronology: Palaeogeography, Palaeoclimatology, Palaeoecology, v. 208, p. 85–102.

NEWTON, R.J., PEVITT, E.L., WIGNALL, P.B., and BOTTRELL, S.H., 2004, Large shifts in the isotopic composition of seawater sulphate across the Permo-Triassic boundary in northern Italy: Earth and Planetary Science Letters, v. 218, p. 331–345.

NÜTZEL, A., 2005, A new Early Triassic gastropod genus and the recovery of gastropods from the Permian/Triassic extinction: Acta Palaeontologica Polonica, v. 50, p. 19–24.

OGG, J., 2004, Overview of global boundary stratotype sections and points (GSSP's), International Commission on Stratigraphy, 17 p., 251kb. <http://www2.udec.cl/geologia/escala/TablaLowerBoundariesGeologicStagesGSSPs_2004.pdf> [Checked 10-10-05].

OJI, T., OGAYA, C., and SATO, T., 2003, Increase of shell-crushing predation recorded in fossil shell fragmentation: Paleobiology, v. 29, p. 520–526.

OTT, E., 1972, Die Kalkalgen-Chronologie der alpinen Mitteltrias in Angleichung an die Ammoniten-Chronologie: Neues Jarbuch fuer Geologie und Palaeontologie, Abhandlungen, v. 141, p. 81–115.

PAN, H.Z., and ERWIN, D.H., 1994, Gastropod diversity patterns in south China during the Chihsia–Ladinian and their mass extinction: Paleoworld, v. 4, p. 249–259.

PAYNE, J.L., 2005, Evolutionary dynamics of gastropod size across the end-Permian extinction and through the Triassic recovery interval: Paleobiology, v. 31, p. 269–290.

PAYNE, J.L., LEHRMANN, D.J., WEI, J.Y., ORCHARD, M.J., SCHRAG, D.P., and KNOLL, A.H., 2004, Large perturbations of the carbon cycle during recovery from the end-Permian extinction: Science, v. 305, p. 506–509.

PRICE-LLOYD, N., and TWITCHETT, R.J., 2002, The Lilliput effect in the aftermath of the end-Permian mass extinction event: Geological Society of America Abstracts with Programs, v. 34, p. 355.

PRONINA-NESTELL, G.P., and NESTELL, M.K., 2001, Late Changhsingian foraminifers of the northwestern Caucasus: Micropaleontology, v. 47, p. 205–234.

PRUSS, S.B., 2004, Lower Triassic microbialites and their relationship to long-term environmental stress following the end-Permian mass extinction: Geological Society of America Abstracts with Programs, v. 36, p. 182.

PRUSS, S., and BOTTJER, D.J., 2004a, Early Triassic trace fossils of the western United States and their implications for prolonged environmental stress from the end-Permian mass extinction: PALAIOS, v. 19, p. 551–564.

PRUSS, S.B., and BOTTJER, D.J., 2004b, Late Early Triassic microbial reefs of the western United States: a description and model for their deposition in the aftermath of the end-Permian mass extinction: Palaeogeography, Palaeoclimatology, Palaeoecology, v. 211, p. 127–137.

PRUSS, S., FRAISER, M., and BOTTJER, D.J., 2004, Proliferation of Early Triassic wrinkle structures: implications for environmental stress following the end-Permian mass extinction: Geology, v. 32, p. 461–464.

RAMOVŠ, A., 1996, Crinoids in Lower Triassic in Slovenia: Albertiana, v. 17, p. 22–24.

RAMPINO, M.R., and ADLER, A.C., 1998, Evidence for abrupt latest Permian mass extinction of foraminifera: results of tests for the Signor-Lipps effect: Geology, v. 26, p. 415–418.

RAMPINO, M.R., PROKOPH, A., and ADLER, A., 2000, Tempo of the end-Permian event: high-resolution cyclostratigraphy at the Permian–Triassic boundary: Geology, v. 28, p. 643–646.

REINHARDT, J.W., 1988, Uppermost Permian reefs and Permo-Triassic sedimentary facies from the southeastern margin of Sichuan Basin, China: Facies, v. 18, p. 231–288.

RETALLACK, G.J., 1999, Postapocalyptic greenhouse paleoclimate revealed by earliest Triassic paleosols in the Sydney Basin, Australia: Geological Society of America Bulletin, v. 111, p. 52–70.

RETALLACK, G.J., 2001, A 300-million-year record of atmospheric carbon dioxide from fossil plant cuticles: Nature, v. 411, p. 287–290.

RETALLACK, G.J., 2002, *Lepidopteris callipteroides*, an earliest Triassic seed fern of the Sydney Basin, southeastern Australia: Alcheringa, v. 26, p. 475–500.

RETALLACK, G.J., VEEVERS, J.J., and MORANTE, R., 1996, Global coal gap between Permian–Triassic extinction and Middle Triassic recovery of peat-forming plants: Geological Society of America Bulletin, v. 108, p. 195–207.

RIDING, R., 2000, Microbial carbonates: the geological record of calcified bacterial-algal mats and biofilms: Sedimentology, v. 47, p. 179–214.

RIEDEL, P., and SENOWBARI-DARYAN, B., 1991, Pharetronids in Triassic reefs: *in* Reitner, J., and Keupp, H., eds., Fossil and Recent Sponges: Springer, Berlin, p. 465–476.

RODLAND, D.L., and BOTTJER, D.J., 2001, Biotic recovery from the end-Permian mass extinction: behavior of the inarticulate brachiopod *Lingula* as a disaster taxon: PALAIOS, v. 16, p. 95–101.

RUSSO, F., MASTANDREA, A., STEFANI, M., and NERI, C., 2000, Carbonate facies dominated by syndepositional cements: a key component of Middle Triassic platforms. The Marmolada case history (Dolomites, Italy): Facies, v. 42, p. 211–226.

RUSSO, F., NERI, C., MASTANDREA, A., and BARACCA, A., 1997, The mud mound nature of the Cassian platform margins of the Dolomites. A case history: the Cipit boulders from Punta Grohmann (Sasso Piatto Massif, Northern Italy): Facies, v. 36, p. 25–36.

SALAJ, J., BORZA, K., and SAMUEL, O., 1983, Triassic Foraminifers of the West Carpathians: Geologický ústav Dionýza Štúra, Bratislava, 213 p.

SANO, H., and NAKASHIMA, K., 1997, Lowermost Triassic (Griesbachian) microbial bindstone-cementstone facies, southwest Japan: Facies, v. 36, p. 1–24.

SCHMIDT-NIELSEN, K., 1984, Scaling, Why is Animal Size so Important?: Cambridge University Press, New York, 241 p.

SCHUBERT, J.K., and BOTTJER, D.J., 1992, Early Triassic stromatolites as post mass extinction disaster forms: Geology, v. 20, p. 883–886.

SCHUBERT, J.K., and BOTTJER, D.J., 1995, Aftermath of the Permian–Triassic mass extinction event—paleoecology of Lower Triassic carbonates in the western USA: Palaeogeography, Palaeoclimatology, Palaeoecology, v. 116, p. 1–39.

SCHUBERT, J.K., KIDDER, D.L., and ERWIN, D.H., 1997, Silica-replaced fossils through the Phanerozoic: Geology, v. 25, p. 1031–1034.

SENOWBARI-DARYAN, B., and FLÜGEL, E., 1993, *Tubiphytes* Maslov, an enigmatic fossil: classification, fossil record and significance through time, Part I: discussion of Late Paleozoic material: *in* Barattolo, F., De Castro, P., and Parente, M., eds., Studies on Benthic Algae: Bolletino della Societa Paleontologica Italiana Special Issue 1, p. 353–382.

SENOWBARI-DARYAN, B., ZÜHLKE, R., BECHSTAEDT, T., and FLÜGEL, E., 1993, Anisian (Middle Triassic) buildups of the Northern Dolomites (Italy); the recovery of reef communities after the Permian/Triassic crisis: Facies, v. 28, p. 181–256.

SEPKOSKI, J.J., JR., 2002, A compendium of fossil marine animal genera: Bulletins of American Paleontology, v. 363, p. 1–560.

SHEN, J.W., KAWAMURA, T., and YANG, W.R., 1998, Upper Permian coral reef and colonial rugose corals in northwest Hunan, South China: Facies, v. 39, p. 35–65.

SHEN, S., and SHI, G.R., 1996, Diversity and extinction patterns of Permian Brachiopoda of South China: Historical Biology, v. 12, p. 93–110.

STANLEY, G.D., 1988, The history of early Mesozoic reef communities: a three-step process: PALAIOS, v. 3, p. 170–183.

STANLEY, S.M., 1990, Delayed recovery and the spacing of major extinctions: Paleobiology, v. 16, p. 401–414.

TWITCHETT, R.J., 1999, Palaeoenvironments and faunal recovery after the end-Permian mass extinction: Palaeogeography, Palaeoclimatology, Palaeoecology, v. 154, p. 27–37.

TWITCHETT, R.J., 2001, Incompleteness of the Permian–Triassic fossil record: a consequence of productivity decline?: Geological Journal, v. 36, p. 341–353.

TWITCHETT, R.J., KRYSTYN, L., BAUD, A., WHEELEY, J.R., and RICHOZ, S., 2004, Rapid marine recovery after the end-Permian mass-extinction event in the absence of marine anoxia: Geology, v. 32, p. 805–808.

TWITCHETT, R.J., LOOY, C.V., MORANTE, R., VISSCHER, H., and WIGNALL, P.B., 2001, Rapid and synchronous collapse of marine and terrestrial ecosystems during the end-Permian biotic crisis: Geology, v. 29, p. 351–354.

TWITCHETT, R.J., WIGNALL, P.B., and BENTON, M.J., 2000, Discussion on Lazarus taxa and fossil abundance at times of biotic crisis: Journal of the Geological Society, v. 157, p. 511–512.

WEIDLICH, O., BERNECKER, M., and FLUGEL, E., 1993, Combined quantitative analysis and microfacies studies of ancient reefs; an integrated approach to Upper Permian and Upper Triassic reef carbonates (Sultanate of Oman): Facies, v. 28, p. 115–144.

WIGNALL, P.B., and BENTON, M.J., 1999, Lazarus taxa and fossil abundance at times of biotic crisis: Journal of the Geological Society of London, v. 156, p. 453–456.

WIGNALL, P.B., and BENTON, M.J., 2000, Discussion on Lazarus taxa and fossil abundance at times of biotic crisis—Reply: Journal of the Geological Society of London, v. 157, p. 512–512.

WIGNALL, P.B., and HALLAM, A., 1992, Anoxia as a cause of the Permian–Triassic mass extinction—facies evidence from northern Italy and the western United States: Palaeogeography, Palaeoclimatology, Palaeoecology, v. 93, p. 21–46.

WIGNALL, P.B., and HALLAM, A., 1993, Griesbachian (earliest Triassic) paleoenvironmental changes in the Salt Range, Pakistan and Southeast China and their bearing on the Permo–Triassic mass extinction: Palaeogeography, Palaeoclimatology, Palaeoecology, v. 102, p. 215–237.

WIGNALL, P.B., and HALLAM, A., 1996, Facies change and the end-Permian mass extinction in SE Sichuan, China: PALAIOS, v. 11, p. 587–596.

WIGNALL, P.B., MORANTE, R., and NEWTON, R., 1998, The Permo-Triassic transition in Spitsbergen: $\delta^{13}C_{org}$ chemostratigraphy, Fe and S geochemistry, facies, fauna and trace fossils: Geological Magazine, v. 135, p. 47–62.

WIGNALL, P.B., and TWITCHETT, R.J., 1999, Unusual intraclastic limestones in Lower Triassic carbonates and their bearing on the aftermath of the end-Permian mass extinction: Sedimentology, v. 46, p. 303–316.

WIGNALL, P.B., and TWITCHETT, R.J., 2002, Extent, duration, and nature of the Permian-Triassic superanoxic event: *in* Koeberl, C., and MacLeod, K.G., eds., Catastrophic Events and Mass Extinctions: Impacts and Beyond: Geological Society of America Special Paper 356, p. 395–413.

WOODS, A.D., BOTTJER, D.J., MUTTI, M., and MORRISON, J., 1999, Lower Triassic large sea-floor carbonate cements: their origin and a mechanism for the prolonged biotic recovery from the end-Permian mass extinction: Geology, v. 27, p. 645–648.

YANG, W., and LEHRMANN, D.J., 2003, Milankovitch climatic signals in Lower Triassic (Olenekian) peritidal carbonate successions, Nanpanjiang Basin, South China: Palaeogeography, Palaeoclimatology, Palaeoecology, v. 201, p. 283–306.

ZONNEVELD, J.-P., MACNAUGHTON, R.B., and PEMBERTON, S.G., 2002, Ichnology and sedimentology of the Lower Montney Formation (Lower Triassic), Kahntah River and Ring Border fields, Alberta and British Columbia: Canadian Society of Petroleum Geologists Abstracts with Programs, p. 355.

ACCEPTED MAY 10, 2005